



## An Observing Night as Seen from the Other Side

*D. Hofstadt, ESO*

It is a major challenge for the technical staff at La Silla to handle experimental and unique type of equipments rather than well-tested commercial machines. But it is an art to deal with a particular species which is just as unique and very peculiar indeed: the astronomer.

The evolution of instrumentation technology has been most unkind to the observer. Nowadays all sorts of sophisticated gadgets are used to collect his photons. Occasionally they ruin his programme. But most disturbing of all is the fact that a little man of growing importance is now taking part in the observation media: the maintenance man.

At night when the instrument fails, hell is breaking loose at the telescope. A fearful little man with a red box is marching into the dome. Immediately confronted with a mass of contradictions, he will have to pave his way to some solid fault evidence. He will be assaulted by a storm of heated queries and complaints.

Why is he coming so late? Couldn't this be prevented? How long will it take to fix the problem? What is wrong anyway?

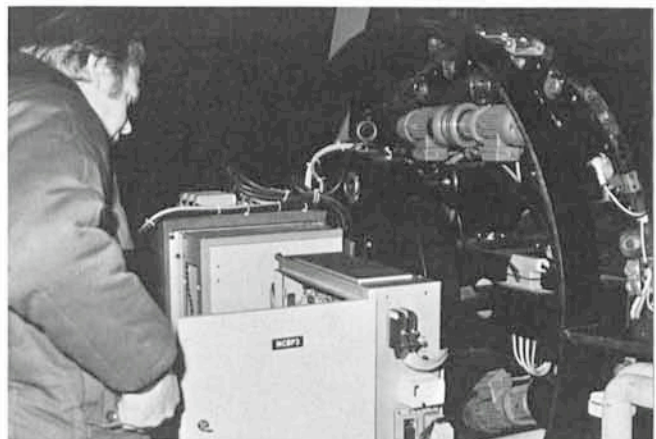
If only he knew! The little man is bracing himself. He knows he must stay calm and inspire confidence for the astronomer does not give him credit as a supreme act of faith. Above all he must display tools and activity. No time to think calmly or study the problem in a quiet place. Physical presence is expected. Else he might have to face interferences, tamperings, hot voices and even disorderly conducts.

Already the news are peddled over the mountain and several foreign faces are sniffing around, commenting the event, commenting the service, commenting the organization.

Gregarious comfort for the victim while the little man is still fiddling with the machine. In front flickering lights refuse to reveal their secret. Behind a tense and nervous face is forwarding more queries. Slowly he feels overcome by blasphemous thoughts.

At last he locates the speck of dust and the instrument starts rattling again.

The little man retreats, relieved and light hearted . . . until his beep, beep is calling again.



*"At night, when the instrument fails . . ."*

## The European Coordinating Facility for the Space Telescope

On 26 June, ESO was chosen by ESA to be the host institute for the Space Telescope European Coordinating Facility. There were three other candidates: the Royal Observatory at Edinburgh, the Institute of Space Astrophysics at Frascati (Italy) and the Institut d'Astrophysique and the Observatoire de Paris in a joint proposal.

The major tasks of the Coordinating Facility will be:

- to provide information to prospective observers of observing programmes;
- to coordinate the development of data analysis software and to create additional software in response to the wishes of the European Space Telescope community;
- to archive and catalogue all Space Telescope observations and to make them available to European Scientists;
- to provide facilities for the reduction of the Space Telescope data by European observers.

P. V.

# The Hubble-Sandage Variable HDE 269006: A Hot Supergiant with a Cool Envelope

*I. Appenzeller, O. Stahl and B. Wolf, Landessternwarte Heidelberg*

## I. Motivation and Observations

The class of bright blue variable stars, which we call "Hubble-Sandage" or "S Dor" variables, contains some of the most luminous stars known in the universe. At maximum light at least their visual brightness may surpass that of any known non-variable star. Because of their high luminosity and since these stars can be distinguished from faint galactic foreground stars by their particular light curves, the identification of such objects in extragalactic systems is relatively easy, and a considerable number of these stars has been discovered in nearby galaxies. Since they can be detected over so large distances, Hubble-Sandage variables could in principle provide a useful tool in the calibration of the extragalactic distance scale and in studies of the physical conditions in extragalactic systems. However, before such investigations can be considered, we first have to learn much more about the nature and structure of these stars. Since all these objects are blue and since as a rule Hubble-Sandage variables are surrounded by dense expanding circumstellar envelopes, spectroscopic observations at ultraviolet wavelengths (where the most common ions in these envelopes have their strongest spectral lines) are particularly important for clarifying the nature of these stars. Therefore, we used the International Ultraviolet Explorer (IUE) satellite to observe some of these objects. In addition we used the ESO observatory at La Silla to supplement the



Fig. 1: The location of the two known Hubble-Sandage variables in the Large Magellanic Cloud. S Dor is in the bright nebulosity near the centre of the image, HDE 269006 is in the lower right-hand (= SW) part. Both stars are indicated by arrows. (Photograph by R. Knigge, 10 inch Metcalf Refractor, Boyden Observatory).

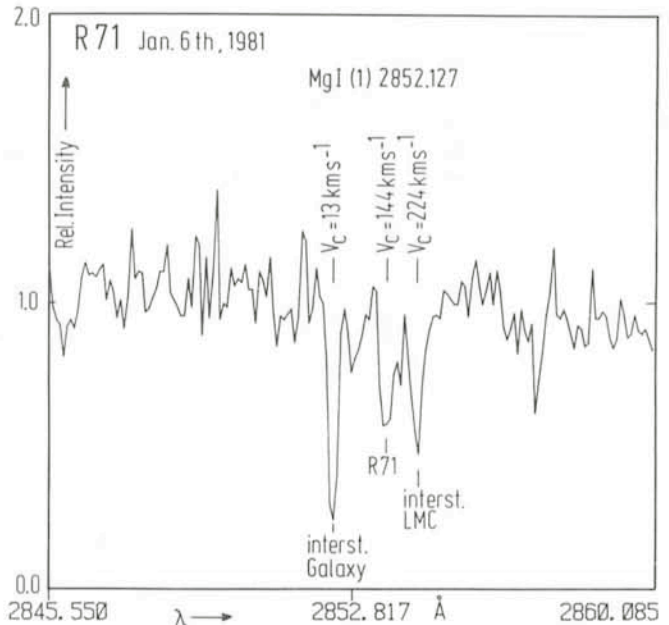


Fig. 2: The Mg I (1) resonance line in the minimum state spectrum of HDE 269006 = R 71. Because of the high photospheric temperature, there is practically no photospheric contribution to this feature. The absorption component at  $v = 144 \text{ km s}^{-1}$  is produced by the expanding circumstellar envelope, while the other two components are due to interstellar gas in our Milky Way galaxy and in the LMC. Note the different strength of the two interstellar components.

satellite observations with ground-based spectroscopic data obtained at the same epoch as the IUE observations. As described in detail below, it was just this possibility of doing (almost) simultaneous observations from space and from the ground that made firm conclusions on at least some aspects of these stars possible.

Although several S Dor-like variables are known in our Milky Way galaxy (notably the peculiar object  $\eta$  Car), light extinction by interstellar dust in the galactic plane (which is particularly strong in the UV) makes UV spectroscopy of these galactic objects difficult. Fortunately, in our neighbouring Large Magellanic Cloud (LMC) galaxy two relatively bright Hubble-Sandage variables are known, which are less affected by interstellar dust extinction. One of these two is the star S Dor which is located close to the centre of the LMC. S Dor was the first Hubble-Sandage variable to be discovered (in 1897 by Pickering), and it is for this reason that many authors prefer to call this class of variable stars the "S Doradus variables". S Dor also was the first star of this type to be investigated by us with the IUE satellite. However, since our results on S Dor have already been published (cf. Wolf, Appenzeller, and Cassatella 1980, *Astronomy and Astrophysics*, **88**, 15) they will not be included in this short report. The second known Hubble-Sandage variable in the LMC is the star HDE 269006 or "R 71". (The latter and shorter designation is its number in the Radcliffe catalogue of bright LMC stars.) R 71 was identified as an S Dor-type variable by Thackeray in 1974. In contrast to S Dor, R 71 is located at a considerable distance from the centre of the LMC (cf. Figure 1), but its radial velocity definitely proves that R 71 is a member of the LMC. As noted already by Thackeray, the

properties of S Dor and R 71 (including their spectra) are strikingly similar (if observed at the same lightcurve phase!), except for the fact that R 71 has a hotter photosphere. Like other Hubble-Sandage variables R 71 shows a lightcurve which (although being clearly not strictly periodic) consists of extended maximum and minimum phases, lasting typically about a decade, separated by relatively short transition periods. The last maximum phase of R 71 occurred between about 1970 and 1977, when the star had a visual magnitude of about  $m_v = 9.9$ . Since sometime in 1978 (when the IUE satellite was launched) R 71 is again in its minimum state, fluctuating slightly around  $m_v = 10.9$ . Although this is rather faint for high-resolution spectroscopy with the IUE satellite (which after all has only a 45 cm telescope) we knew that the star is relatively hot (photospheric spectral type during the minimum state: B 2.5 Iep) and we therefore expected such observations to be just possible. Indeed, two very long IUE exposures, each lasting more than seven hours, obtained in January 1981, resulted in two well-exposed high-resolution spectrograms, which together cover the wavelength range 1250 to 3200 Å. Coudé spectrograms obtained at the ESO 1.5 m telescope at the same epoch cover the wavelength range 3550 to 4900 Å. For technical reasons it was not possible to take simultaneously spectrograms in the red spectral range. However, for completeness, one week earlier we had obtained several low-resolution image-tube spectrograms of R 71 covering the wavelength range 5400 to 7000 Å. These plates showed that at least the basic properties of the red spectrum had remained unchanged since our high-resolution spectroscopic observations of the  $H_{\alpha}$  region carried out 14 months earlier at the beginning of the

## Tentative Time-table of Council Sessions and Committee Meetings

November 10	Scientific Technical Committee
November 11 – 12	Finance Committee
November 13	Committee of Council
Nov. 30 – Dec. 1 – 2	Observing Programmes Committee
December 3 – 4	Council

All meetings will take place at ESO in Garching.

present minimum of R 71. The spectroscopic observations were supplemented by photometric observations which Dr. S. Wramdemark kindly carried out for us at ESO.

## II. Results

There are two main results of our coordinated IUE and ground-based observations of R 71: Firstly, our observations allowed to derive the continuum energy distribution of R 71 for all wavelengths which contribute significantly to the total luminosity of this star. From an integration of the energy distribution and from the known distance of the LMC we were able to calculate the (minimum state) total luminosity of R 71 which was found to be about 200,000 times the solar luminosity. In addition, the shape of the energy distribution allowed us to estimate the photospheric effective temperature (about

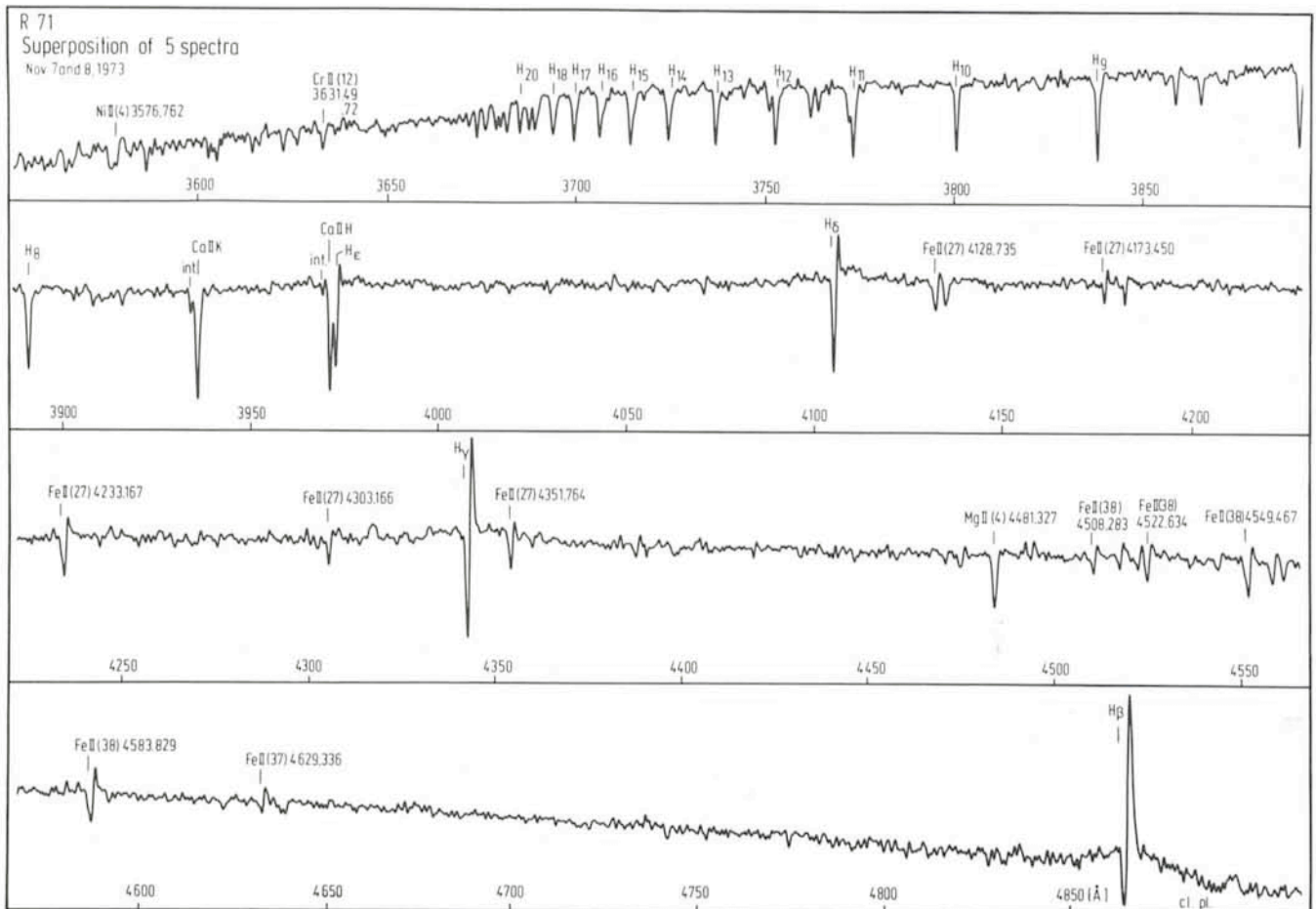


Fig. 3: The photographic maximum state spectrum of HDE 269006.

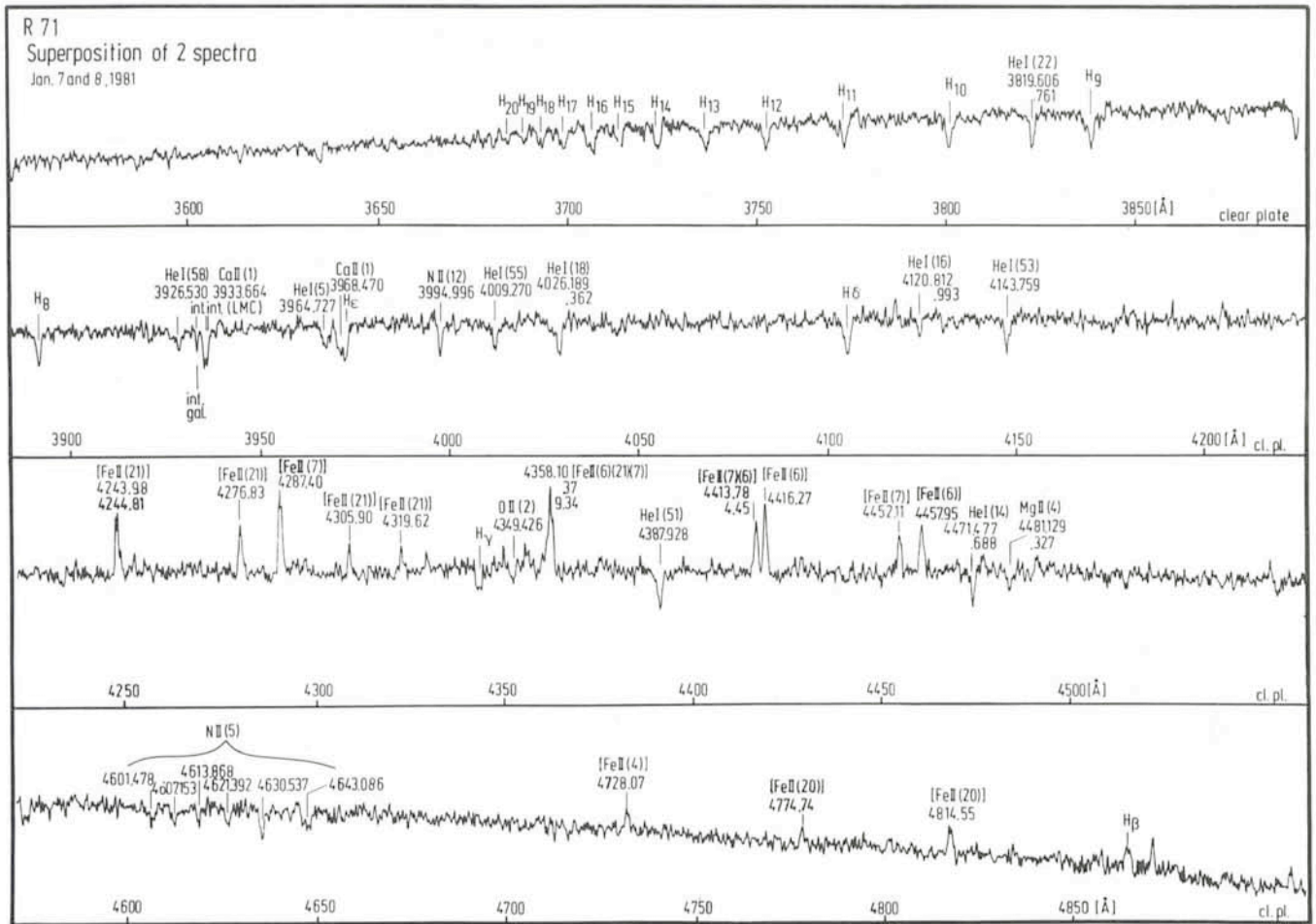


Fig. 4: The photographic minimum state spectrum of HDE 269006.

14,000 K). Although the luminosity quoted above is huge, it is considerably lower than had been expected from ground-based observations alone. In part this difference is due to the (for a B 2.5 star) relatively low effective temperature. However, more important is the fact that as a result of numerous broad envelope absorption lines of many different ions, the ultraviolet flux of R 71 was found to be much lower than expected.

In passing we note that for the derivation of the total luminosity and effective temperature we first had to estimate the total light extinction by interstellar dust along the line of sight to R 71. From earlier ground-based observations of distant galactic stars and "normal" LMC stars the galactic foreground extinction in the direction of R 71 was known to be relatively small ( $E_{B-V} \approx 0.05$ ). However, the additional extinction occurring inside the LMC was unknown. Although our spectroscopic observations did not allow to detect this dust extinction directly, we were able to observe many interstellar absorption lines produced by the interstellar gas in the LMC. Because of the orbital motion of the solar neighbourhood around the centre of our galaxy, these lines are redshifted compared to their galactic counterparts and can therefore be separated on high-resolution spectrograms. As illustrated by Figure 2 (and also by the  $\lambda$  2599 line, Figure 5) the LMC interstellar lines were always found to be weaker than those produced in our galaxy, indicating that along the line of sight to R 71 there is even less interstellar matter in the LMC than in our galaxy.

A second important result of our observations concerns the properties of the circumstellar envelope of R 71, as derived from the UV and visual line spectrum: In Figure 3 and 4 we give, respectively, the maximum state and the minimum state line

spectrum in the wavelength range 3550 to 4900 Å. (The maximum state spectrum was observed by M. de Groot in 1973 and will be described in detail in a forthcoming publication by Stahl, Bastian, de Groot, and Wolf.) Both spectra reproduced in Figures 3 and 4 are based on coude plates obtained at ESO, with the same equipment, and all plates were reduced in the same way. As shown by Figure 3, the maximum state spectrum is dominated by emission lines of hydrogen and the permitted multiplets of Fe II, Cr II, Ni II, etc. All emission lines show pronounced "P Cygni line profiles" (i.e. absorption components bluewards of the emission peaks). In addition there are blueshifted strong absorption lines (like the Ca II H and K lines). The P Cygni line profiles and the 3 blueshifted absorption lines are obviously produced in matter moving away from the star, i.e. in the expanding circumstellar envelope. The (rather weak) high excitation He I, Mg II, and Si II lines, which are formed in the deeper layers of the photosphere, are unshifted.

At minimum light (Figure 4) the blue-visual spectrum of R 71 looks highly different: In the whole spectral range reproduced, there is no line showing a P Cygni profile, and the once dominant permitted Fe II, Cr II, and Ni II emission lines are undetectable or extremely weak. Instead, the (unshifted) high excitation photospheric lines are now rather conspicuous in absorption. In addition, the spectrum now is dominated by forbidden [Fe II] emission lines of considerable strength (although such lines are undetectable in the maximum state spectrum). However, the greatest surprise came when we looked at the high-resolution IUE spectrograms obtained simultaneously with the spectrum reproduced in Figure 4. As

illustrated by Figure 5, in the far ultraviolet part of the spectrum, permitted Fe II lines are still present (and in fact quite strong) and show beautiful P Cygni line profiles! Other sections of the UV spectrum contain many more P Cygni profiles or blue-shifted absorption lines of many different ions ranging from Mg I to C IV, proving that the outflowing circumstellar envelope is still present in the minimum state. However, a closer look showed that only envelope lines of relatively low excitation potential could be detected (throughout the spectrum). From a comparison of the different line strengths we found for the envelope a rather cool excitation temperature of only about 6,000 K. This obviously explains the absence of the permitted metallic lines in the photographic minimum state spectrum, since all these lines in the photographic wavelength range originate from energy levels not significantly populated at such low temperatures.

Since forbidden lines are emitted only from highly rarefied gases, it is clear that the [Fe II] lines shown in Figure 4 must originate at a considerable distance from the stellar photosphere. A simple analysis of the observed line strengths indicates for this region a distance of about 100 stellar radii. Therefore, we can use the width of the [Fe II] lines to estimate the expansion velocity of the envelope at this distance to  $78 \pm 6 \text{ km s}^{-1}$ . On the other hand, from the P Cygni profiles (which can be formed only within a few stellar radii from the star) of the permitted UV Fe II lines, we can estimate the expansion velocity close to the stellar surface to about  $127 \text{ km s}^{-1}$ . Thus, R 71 seems to have a *decelerated* expanding circumstellar envelope, which is thought to be rather unusual for luminous early-type stars. By comparing the observed P Cygni profiles of the Fe II lines to model computation we furthermore estimated

## Applications for Observing Time at La Silla

Period 29

(April 1 to October 1, 1982)

Please do not forget that your proposals should reach the  
Section Visiting Astronomers **before October 15, 1981.**

the minimum state mass loss rate of R 71 to  $3 \times 10^{-7}$  solar masses per year, compared to a maximum state mass loss of the order of  $5 \times 10^{-5}$  solar masses per year. On the other hand, we found the expansion velocity of the envelope to be about the same at maximum and minimum state. This can be understood only under the assumption that the density of the envelope at maximum light is higher by a factor of the order of 100 or more. This suggests that the density of the circumstellar envelope is probably the main difference between the minimum and maximum state of R 71. The higher visual brightness of the maximum state would then simply be due to the fact that more of the photospheric ultraviolet radiation is absorbed by the envelope and reradiated at visual wavelengths. An excellent test of this hypothesis would be a direct comparison with IUE spectrograms of R 71 obtained at maximum state. Unfortunately, as noted above, the last maximum had just ended when the IUE satellite was launched, and a comparison of the average duration of the minimum state of R 71 and of the estimated life expectancy of the IUE satellite makes it questionable whether such observations will ever become possible.

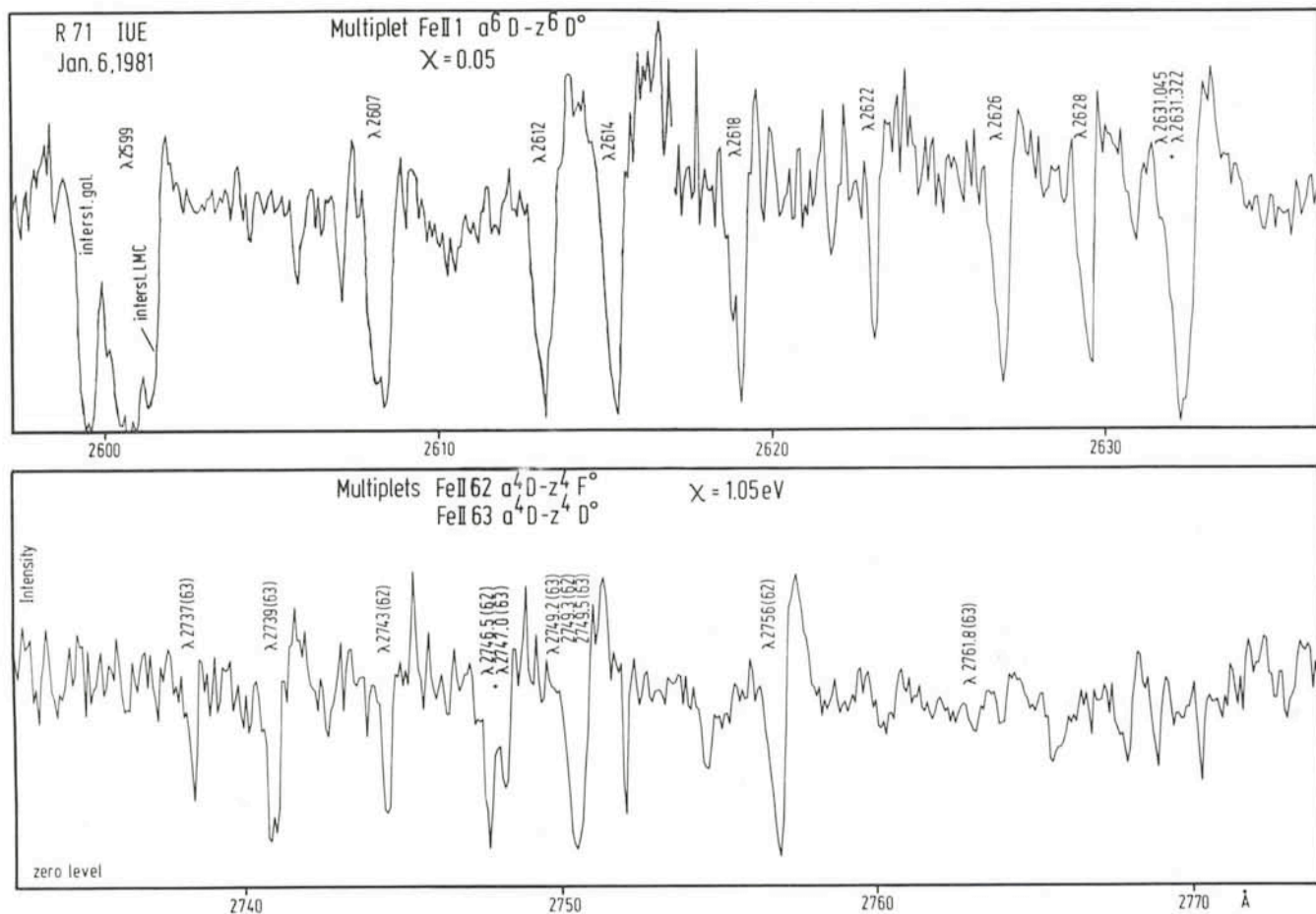


Fig. 5: Sections of the minimum state UV spectrum of HDE 269006, showing examples of the P Cygni profiles of the low excitation Fe II I

# First Observations with CORAVEL at La Silla

M. Imbert and L. Prévot, Observatoire de Marseille

*CORAVEL is a spectrometer specialized for the determination of stellar radial velocities with very high time resolution and high accuracy. The first instrument has been operational since 1977 on the 1 m Swiss telescope at the Haute-Provence Observatory where nearly 20,000 radial velocity measurements have been made by astronomers from the Geneva and Marseille Observatories. Although a preliminary report on the prototype has been given by M. Mayor (THE MESSENGER No. 8, March 1977) it seems interesting to give further information about the instrument's performance: they are exceptional both for accuracy ( $0.5 \text{ km s}^{-1}$  or better) as well as for high-speed acquisition (measurements in less than 5 min.) and for sensitivity (limiting magnitude  $B > 13$ ). The efficiency of this technique was so impressive that observing programmes in the southern hemisphere far beyond the limit of classical radial velocity spectrographs could be considered. Therefore a second CORAVEL has been installed at the Cassegrain focus of the 1.54 m Danish telescope at La Silla, and observations took place in January-February 1981. The results obtained during this period are quite remarkable.*

## The Instrument

The spectrometer, already described by A. Baranne, M. Mayor and J. L. Poncet (*Vistas in Astronomy*, vol. 23, p. 279, 1979), contains an echelle grating ( $79 \text{ grooves mm}^{-1}$ ) used between orders 43 and 62; it gives a dispersion of  $2 \text{ \AA mm}^{-1}$  and a useful spectral range from  $3700 \text{ \AA}$  to  $5200 \text{ \AA}$ . The spectrum of the star or of the comparison lamp is focused onto a mask containing about 3000 apertures. A scanning plate moves the spectrum with respect to the mask. This produces a variation of the flux which is at a minimum when the absorption lines of the star to be measured are in coincidence with the apertures of the mask. The scanning rate is fixed at  $5 \text{ Hz}$  in order to minimize the effects of atmospheric scintillation. The flux, corresponding to the correlation function between the relative positions of the spectrum and the mask, is measured by means of a photomultiplier. The correlation function is calculated on-line by incrementation in the memory of an HP 21-MX computer. Integrating a number of scans allows determination of the peak of the correlation function which is permanently displayed on a screen; this allows the radial velocity determination with a typical accuracy of  $0.5 \text{ km s}^{-1}$ . The velocity zero-point is determined twice for each exposure, using the spectrum given by an iron hollow-cathode lamp. The heliocentric velocity is computed immediately after the exposure, and all the data are stored on magnetic tape.

The present mask has been made photographically from the spectrum of Arcturus. It allows a range of spectral compatibility from early F to late M types.

## Programmes and First Observations

Undertaking new programmes of major interest implied that CORAVEL should be mounted on a rather large telescope ( $1.5 \text{ m}$  or more) allowing fast automatic pointing. The  $1.54 \text{ m}$  Danish telescope at La Silla was in fact the only instrument well adapted to receive CORAVEL (Fig. 1). Moreover, the bulk of the programmes considered and some technical imperatives required rather long observing periods which could be obtained owing to the use of reserved Danish periods jointly to those allotted by ESO. This has naturally led to a collaboration between several astronomers from several institutes or observatories including, among others, J. Andersen and B. Nordström (Copenhagen), A. Ardeberg and E. Maurice (ESO), M. Mayor (Geneva), M. Imbert and L. Prévot (Marseille). Within the framework of this collaboration, several prime-interest programmes have been defined and should be carried out in a short time. They can be summarized as follows.

(1) Programmes allowing fast data acquisition and requiring a large number of measurements.

– Stars in the Yale Catalogue of Bright Stars: it is necessary to complete the fundamental data of this catalogue, as 850 late-type stars do not yet have radial velocities.

– Population II F-G stars already observed photometrically: more than 200 bright stars need radial velocity measurements to allow the determination of their dynamical trend.



Fig. 1: CORAVEL mounted at the Cassegrain focus of the  $1.54 \text{ m}$  Danish telescope at La Silla.

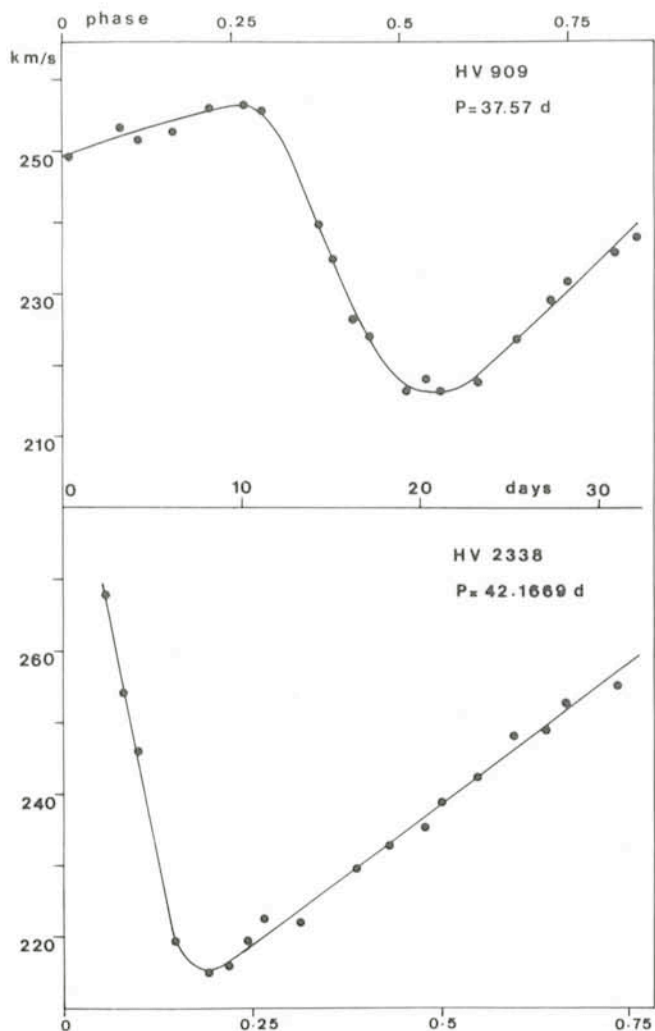


Fig. 2: Radial velocity curves of two cepheids in the Large Magellanic Cloud. The observations cover nearly one cycle; they show the high quality of measurements made on very faint objects ( $B = 14.1$  to  $15.1$  for HV 909 and  $B = 13.8$  to  $14.4$  for HV 2338).

(2) Programmes beyond the limit of classical spectrographic methods:

- Individual radial velocities of 350 stars in the globular clusters  $\omega$  Cen and 47 Tuc, for which a few poor quality velocities exist. The main aim concerns the kinematic study of globular clusters and the fit of their velocity fields to theoretical models.

- Pulsations of extragalactic cepheids: this programme concerns 15 LMC and 5 SMC long period cepheids for studying their pulsation modes and determining their radii.

- Radial velocities in the Magellanic Clouds: 400 LMC and 150 SMC red supergiants must be observed in order to go further into the knowledge of the Population I velocity fields in these galaxies.

A first period of observations (January-February 1981) allowed us to obtain 1,500 radial velocities for stars up to  $B = 15.3$ , with an accuracy of around  $1 \text{ km s}^{-1}$  for the faintest objects. We were able to undertake all programmes and none of them has proved unfeasible. Most of the bright stars have been measured once; this represents several hundreds of new radial velocities. High velocities have been found for some, among the Population II F-G stars. One hundred and fifty radial velocities have been determined for luminous cepheids in the LMC. The observations cover nearly one cycle for the objects

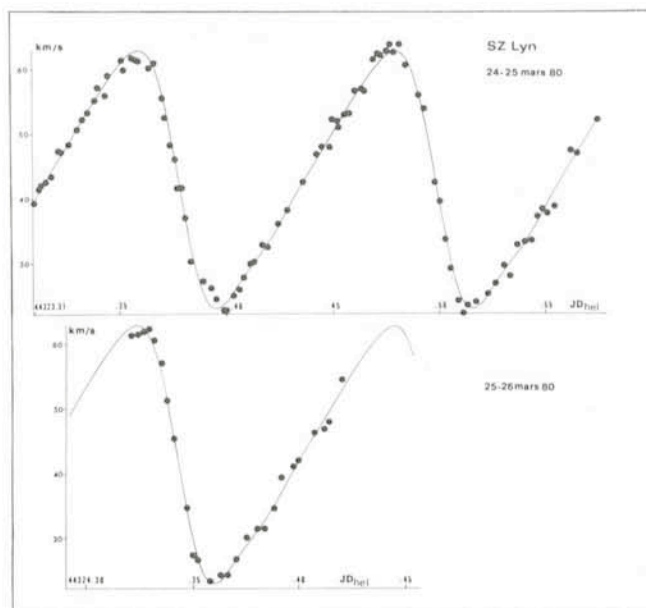


Fig. 3: Another aspect of the performances of CORAVEL, the high time resolution, is illustrated by this figure which reproduces the radial velocity variations of the dwarf cepheid SZ Lyn (Period  $2^{\text{d}}49^{\text{m}}$ ,  $V = 9.2$  to  $9.6$ ) observed at the Haute-Provence Observatory with integration times around 1 min.

of shorter period ( $P = 30$  to  $40$  days). The results show clearly that there exist variations in the amplitudes and in the shapes of the velocity curves for stars of similar periods (Fig. 2). One hundred and fifty red giants were measured in  $\omega$  Cen, some in the centre of the cluster. A rough analysis of the velocities shows a relative complexity of the stellar motions. Around 120 LMC red supergiants were also measured; among them 100 stars were confirmed as members on the basis of radial velocities. Despite their unfavourable position at the time of the observations, some stars in the globular cluster 47 Tuc and in the SMC could be measured in order to prove that these objects are accessible with CORAVEL.

In short, the first observing period (30 nights) has allowed us to obtain an exceptional number of highly accurate radial velocities. Such large and difficult programmes were totally outside the range of the performance of classical instruments. In the near future, two additional periods, already allotted by ESO, will be used to collect additional data for the programmes undertaken, particularly the pulsation of cepheids in the Magellanic Clouds and the kinematics of 47 Tuc.

Thus, the mounting of CORAVEL on a highly automated instrument like the 1.54 m Danish telescope has been a full success. It is hoped that future runs may be as positive and take place with a similar collaboration.

## New Head of the Scientific Division

Professor P. O. Lindblad has resigned as of 31 August from his position as Head of the Scientific Division, following his election to be Director of the Stockholm Observatory.

The Director-General has appointed in his place Professor Giancarlo Setti who will take up his duties on 1 January 1982.

# Clusters of Galaxies

W. K. Huchtmeier and O.-G. Richter, Max-Planck-Institut für Radioastronomie, Bonn  
J. Materne, Institut für Astronomie und Astrophysik, Technische Universität, Berlin

## Introduction

The large-scale structure of the universe is dominated by clustering. Most galaxies seem to be members of pairs, groups, clusters, and superclusters. To that degree we are able to recognize a hierarchical structure of the universe. Our local group of galaxies (LG) is centred on two large spiral galaxies: the Andromeda nebula and our own galaxy. Three smaller galaxies – like M 33 – and at least 23 dwarf galaxies (Kraan-Korteweg and Tammann, 1979, *Astronomische Nachrichten*, **300**, 181) can be found in the environment of these two large galaxies. Neighbouring groups have comparable sizes (about 1 Mpc in extent) and comparable numbers of bright members. Small dwarf galaxies cannot at present be observed at great distances.

Kraan-Korteweg and Tammann associate at least two thirds of the galaxies within 10 Mpc with groups. Other authors give even lower limits to "field" galaxies down to only 1% (Huchra and Thuan, 1977 *Astrophysical Journal*, **216**, 694) on the basis of 1,088 galaxies). The relative proportions of the two populations (field and cluster members) and the difference in their global properties should help in determining the relative influence of the environment on the formation and evolution of a galaxy. Peebles' (1974 *Ap. J.*, **189**, L51) theory of the formation of clusters of galaxies from the gravitational instability of the

early universe suggests that all galaxies should be clustered on all scales and there should be no homogeneous component. This prediction cannot definitively be tested owing to the difficulty in determining the membership of individual galaxies even if good radial velocities are available.

## The Nearest Rich Clusters

The nearest rich cluster is the Virgo cluster at a distance of 15–20 Mpc. Its main body covers an area of  $6^\circ$  in diameter on the sky, corresponding to a linear extent of 2 Mpc. Its mean radial velocity (corrected for the rotation of our galaxy) is  $v_0 \sim 1,100$  km/s. The velocity dispersion is 556 km/s for E and S0 galaxies and 821 km/s for spiral galaxies. These values were derived from about 50 galaxies each. The lower velocity dispersion of the T and S0 galaxies and their greater concentration to the centre of the cluster show that early-type galaxies dominate the inner part of this cluster. Spirals are predominantly found in the outer parts. The more or less smooth distribution of spirals across the area of the Virgo cluster is obviously a projection effect. Beyond the inner  $6^\circ$ , the structure of the Virgo cluster becomes irregular. Outside a circle of  $15^\circ$  diameter, several "clouds" of galaxies are found. The Virgo cluster and all groups from its environment form the local supercluster. This is an elongated and flattened system of

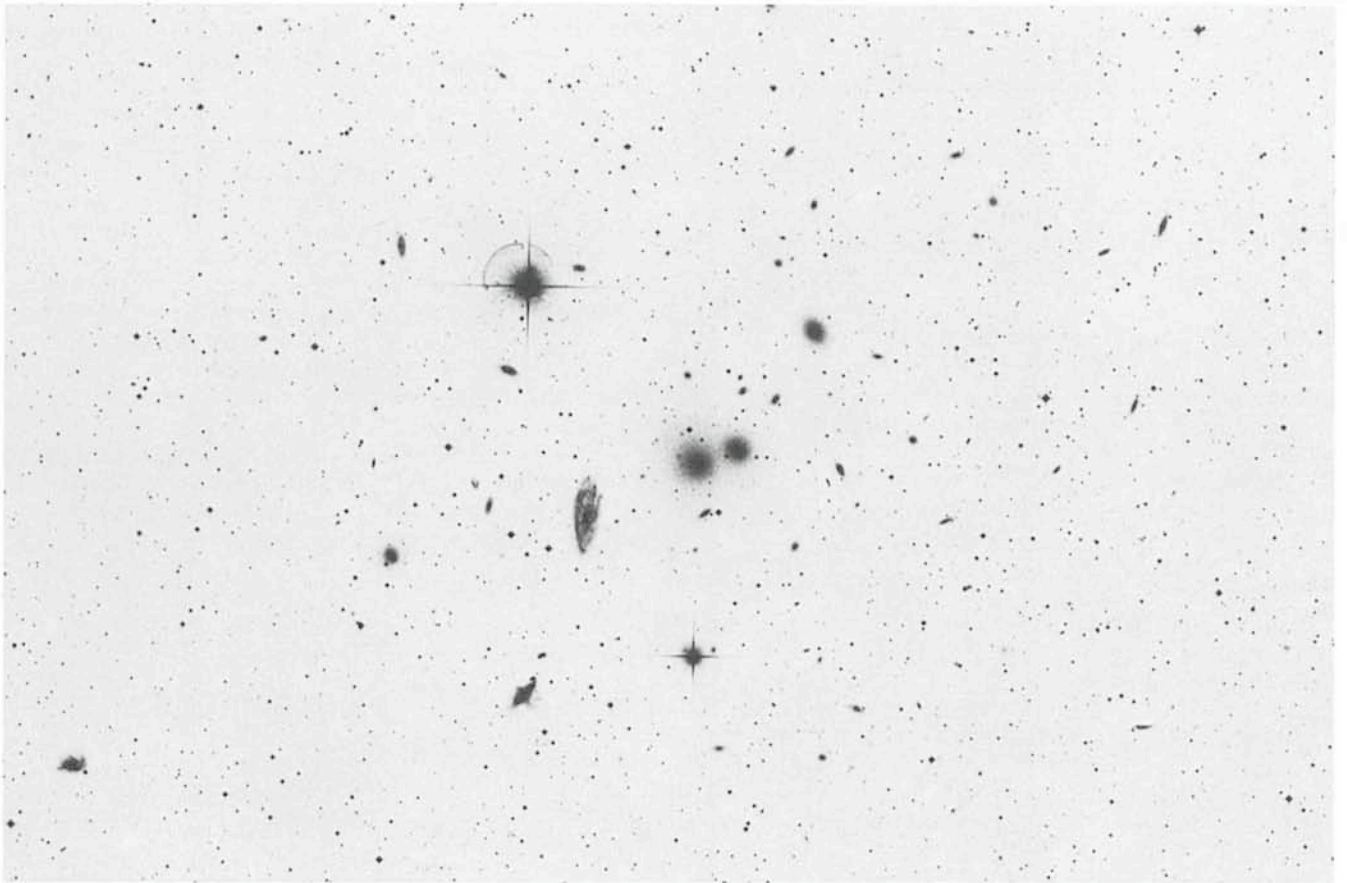


Fig. 1: Central area of the Hydra I cluster of galaxies (reproduced from the ESO B survey). The angular separation of the two central spherical galaxies NGC 3309 (type E1) and NGC 3311 (S0) is 1'.6.

roughly 25–30 Mpc in length and 15 Mpc in width. Most members lie within a few Mpc of the supercluster plane.

Beyond the Virgo cluster, Hydra I (= Abell 1060) is the next in the sequence of spiral-rich clusters (Fig. 1). It has Abell distance class O and richness class 1 and is situated at the eastern edge of the Hydra-Centaurus supercluster. Zwicky first published diagrams of the distribution of its galaxies (1941, *Proc. Nat. Acad. Sci.*, 27, 264). From the observed apparent luminosity function he derived a radial velocity of about 4,000 km/s for the cluster, on the assumption of a constant absolute magnitude for the brightest galaxies in clusters. This value is in reasonable agreement with the radial velocity of 3,400 km/s, derived from our observations in Chile.

The next rich cluster is the regular Coma cluster at a distance of about 90–130 Mpc ( $v_0 = 6,900$  km/s) which is dominated by early-type galaxies (E/S0). The main body of the Coma cluster is contained within a radius of 100' (about 4 Mpc). It is generally assumed that, initially, galaxies of different masses have the same distribution law within a given cluster. Massive galaxies will experience a deceleration due to two-body encounters resulting in mass segregation. In fact, in the central part of the Coma cluster a significant amount of mass segregation is found among the brightest members ( $M > 10^{12} M_{\odot}$ ). Outside this inner part the Coma cluster becomes asymmetric. To the west, an irregular supercluster seems to extend out to about  $14^{\circ}$  (nearly 35 Mpc). Galaxies at such distances have not had time to cross the centre of the cluster, and should therefore roughly reflect the initial conditions of cluster formation.

A structure like that of the Coma cluster is typical for rich regular clusters. Core radii seem to have the same linear values of about 0.4 Mpc for all rich clusters. The centres of rich clusters are often dominated by giant elliptical galaxies: M 87 in Virgo or NGC 4889 in Coma. Several classification schemes have been developed (for a review see e.g. Bahcall, 1977, *Ann. Rev. Astron. Astrophys.*, 15, 505). Some depend on morphology, others on the dominance of bright galaxies or on the galaxy content of clusters. To enter Abell's catalogue, a cluster has to have more than 50 members within a radius of  $3 \cdot h_{50}^{-1} \cdot \text{Mpc}$ , which are brighter than the magnitude of the third brightest galaxy plus two magnitudes. Abell's catalogue contains a total of 2,712 clusters north of declination  $-27^{\circ}5$ .

Galaxy counts<sup>7</sup> within concentric rings around the cluster centre yield the projected surface density distribution and thus information about the relative concentration towards the centre and the regularity of the cluster structure. With the assumption of spherical symmetry the measured surface density can be used to calculate the space density. Such information is available for nearly 150 clusters. More detailed studies, for example of mass segregation and of the distribution of galaxy types, are possible with additional information about morphological types and apparent magnitudes of individual member galaxies. A well defined relationship is found between local galaxy density and the distribution of galaxy types, namely an increasing elliptical and S0 population and a corresponding decrease in spirals with increasing density.

Galaxy counts in the Hydra I cluster (Kwast, 1966, *Acta Astron.*, 16, 45) show a sharp peak of the galaxy density distribution in the centre, stronger than can be explained by an Emden isothermal gas sphere model. Additional information can be obtained from radial velocity measurements. Cluster membership can only be discussed if radial velocities are known. Thus many redshifts are necessary for the computation of elaborate models. Unfortunately the greatest shortage in available data is that of redshifts. Radial velocities of cluster



Fig. 2: A close-up view of the two peculiar spirals NGC 3312 (top) and NGC 3314 (bottom), the latter being a superposition of two spiral galaxies. This 25 min. exposure with the ESO 3.6 m telescope was made on baked IIIa-J + GG 385.

galaxies tell us something about kinematics, which in principle yields information about the gravitational potential, masses, and forces. At present, reasonable numbers of radial velocities – i. e. for more than about 20% of all member galaxies – are available only for very few clusters, among which are those of Virgo, Coma, and Hercules.

As early as 1937 Zwicky realized the “missing-mass” problem when applying the virial theorem to clusters of galaxies. The total mass of clusters derived this way is about 1 to 2 orders of magnitude greater than the sum of the masses of individual galaxies. The missing mass cannot be hidden in the observed galaxies as two-body relaxation then would be fast enough to produce substantial equipartition of energy between light and massive galaxies. Intergalactic gas (neutral gas is not observed) manifests its presence by radio continuum and X-ray emission in a number of clusters. The amount of gas is hardly comparable to the mass observed in galaxies and thus does not solve the missing-mass problem.

## The Hydra I Cluster: Description

In a project to study the properties of nearby medium-sized clusters we observed the Hydra I cluster (Abell 1060), which lies at R.A.  $10^{\text{h}}34^{\text{m}}$  and DEC.  $-27^{\circ}16'$ , using the ESO 1.52 m and 3.6 m telescopes and the 100 m radio telescope of the MPIfR at Effelsberg. The high percentage of spiral galaxies is already evident from Fig. 1. This was one of the reasons to include Hydra I in our project, the aim of which was to derive radial velocities of the spiral galaxy population from 21 cm line observations of neutral hydrogen (HI), to complete the sample of radial velocities, to derive global parameters of the spirals from the HI observations for a detailed comparison with global parameters of the “local sample” of spiral galaxies, i. e. with

<sup>7</sup>  $h_{50} = H_0/50 \text{ km s}^{-1} \text{ Mpc}^{-1}$ ,  $H_0$  = Hubble constant.

galaxies not in clusters, and to study the influence of the cluster environment on the evolution of galaxies. Spiral galaxies in Hydra I contribute about 50% to the total galaxy content. The ratio of spiral to elliptical galaxies increases from 0.2 in the centre up to a value of 4 at a radius of about 4 Mpc. The dwarfs and low surface brightness galaxies follow the spatial distribution of the E-galaxy population. The spirals in the dense part of the cluster are "anemic", lacking gas and star formation as indicated by their reddish colour. This is in agreement with low upper limits of neutral hydrogen. Within the main body of Hydra I upper limits to the  $M_{HI}/L$  ratio of these spirals are of the order of 0.2 or less, compared with an expected  $M_{HI}/L \sim 0.4$ . For NGC 3312 the corresponding value is  $\leq 0.06$ . In contrast, a few spirals on the periphery of Hydra I show a normal HI content. In addition, spirals in the Virgo cluster are HI deficient by a factor of about 2 on the average. Observations of some spirals in the Coma cluster and in Abell 1367 show an HI deficiency by a factor of at least 4 (Sullivan and Johnson, 1978, *Ap. J.*, **225**, 751).

The gravitational centre of Hydra I is close to the two spherical galaxies in the centre, NGC 3309 (E1) and NGC 3311 (S0) (right and left respectively). A large-scale photograph of these two galaxies was already shown in the MESSENGER No. 10. Hydra I is classified by Bautz and Morgan as a type-III cluster and by Rood and Sastry as a type-C cluster, implying a core-halo structure with no dominant galaxy. Hydra I is a cluster X-ray source with a luminosity  $L_x \sim 2 \cdot 10^{43}$  erg/s (in the 2–10 keV range). Solinger and Tucker (1972, *Ap. J.*, **175**, L107)

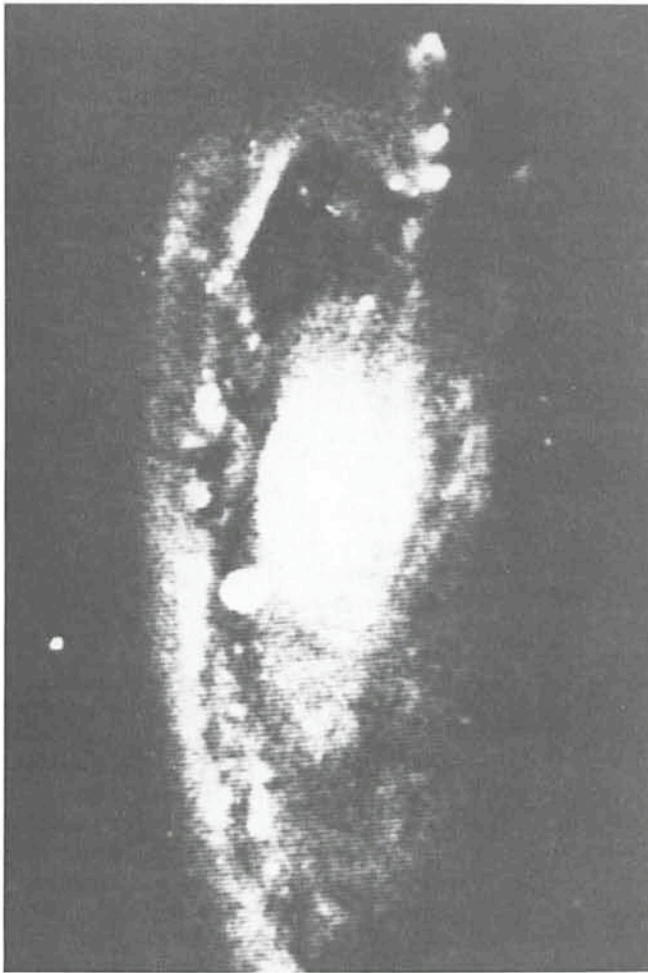


Fig. 3: The isodensity map of NGC 3312 shows an enlarged and contrast-enhanced version of Fig. 2.

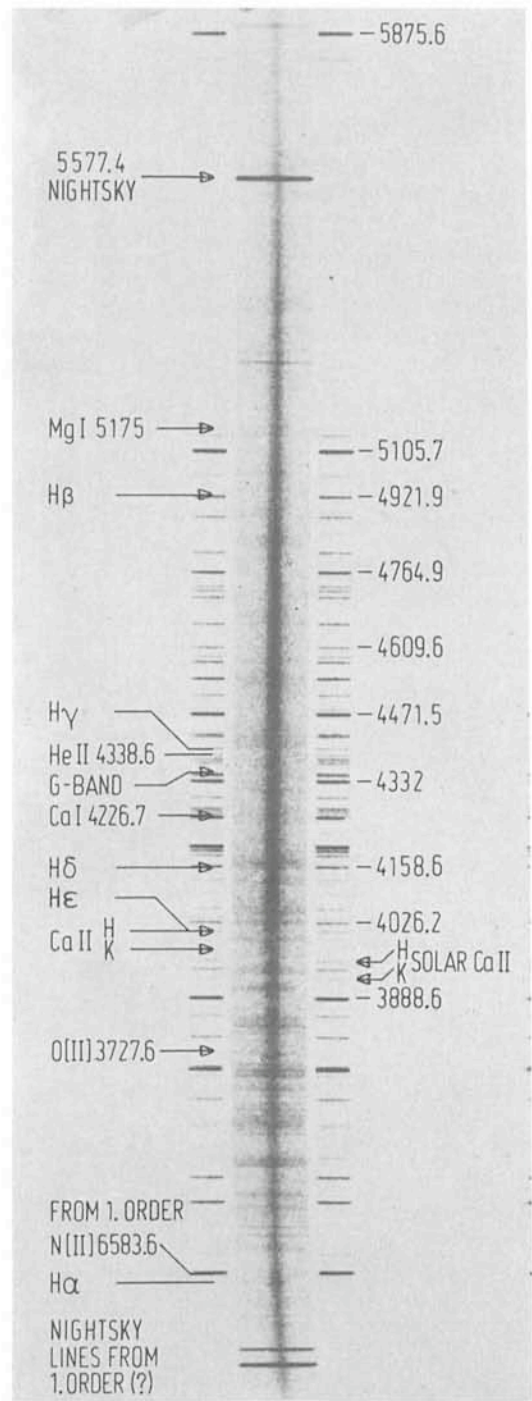


Fig. 4: Spectrum of the edge-on Sb galaxy A1036.3–2818; exposure time 35 min., original dispersion 86 Å/mm. The position angle of the slit was set to the position angle of the galaxy. Note the inclination of the galaxy spectral lines – e.g.  $\lambda$  3727 – along the slit. This gives a direct measure of the rotation of A 1036.3–2818.

suggested that the cluster radial velocity dispersion, which represents a comparatively easily determined measure of the cluster gravitation potential, should be correlated with the cluster X-ray luminosity. On the basis of the X-ray observations the Hydra I cluster is at the low end of the diagram of X-ray luminosity versus velocity dispersion. Because no radio galaxy is known to exist in Hydra I, its X-rays cannot be due to a single active galaxy but must be generated by hot intergalactic gas. Also, the optical appearance of NGC 3312 suggests the existence of dispersed intergalactic matter. Fig. 2 shows the

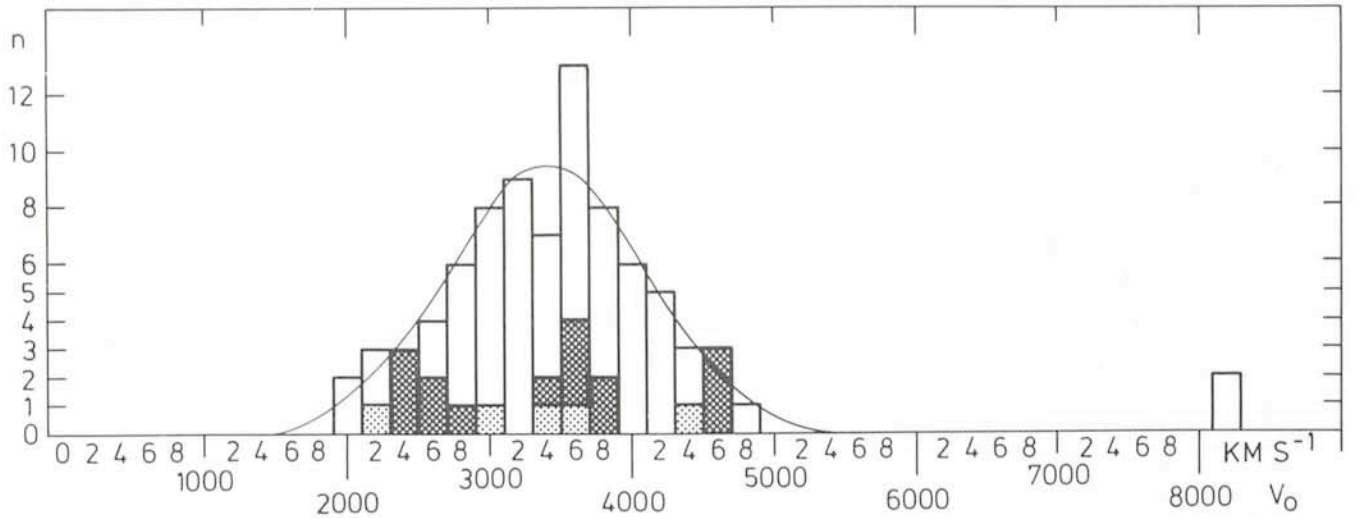


Fig. 5: Histogram of radial velocities of galaxies in the Hydra I field; values from the literature are shaded. The overlap of the older sample and our own measurements is given in lighter shading. The Gaussian fit defines the mean radial velocity of the cluster and its velocity dispersion. Remarkable is the empty space in front and behind Hydra I (at least for  $v_0 < 8,000$  km/s).

bright disturbed spiral galaxy in the core of A1060, which has a linear extent of roughly 40 kpc. An asymmetrical distribution of very faint filamentary features has been detected in blue light extending from the disk of this galaxy to a projected distance of at least 30 kpc. Gallagher (1978, *Ap. J.*, **223**, 386) presented evidence that NGC 3312 is being stripped of its interstellar medium by ram pressure. Fig. 3 shows a contrast-enhanced image of NGC 3312, obtained by scanning the original 3.6 m PF plate with the PDS machine of the Lund Observatory and displaying the image on a TV screen using a logarithmic scale for the gray code.

### The Hydra I Cluster: Observations

Accurate coordinates for more than 1,300 galaxies in the Hydra I field and magnitudes (to  $0^m.2$ ) for a high percentage of them are available. Morphological types and radii are given for about 300 galaxies (R. J. Smyth, 1980, Thesis, ROE). In sharp contrast with this amount of data only 20 redshifts were known up to 1980. In order to derive more radial velocities we used the ESO 1.5 m telescope with the Boller & Chivens spectrograph equipped with an EMI 3-stage image tube during three observing periods in March 1980, May 1980 and April 1981. Spectra were recorded on photographic plates, which is a cheap but

effective procedure. The Grant machine in Geneva was used to measure line positions accurate to about  $0.5 \mu\text{m}$ . All spectra were taken with the same setting of the grating, i.e. the comparison spectrum is always the same. The difficult problem is to recognize and identify the lines in a galaxy spectrum, as they are often very faint and noisy. Furthermore, if only a few lines can be seen, it is difficult to identify them correctly. A sample spectrum is shown in Fig. 4. This way we were able to measure more than 100 radial velocities of galaxies brighter than about  $15^m.5$ , i.e. galaxies up to three magnitudes fainter than the brightest cluster member, and we reached the limit of the ESO 1.5 m telescope.

The distribution of all radial velocities in the Hydra I field, presented as a histogram in Fig. 5, shows a very good definition of cluster membership in velocity space: there are no foreground galaxies in the observed field and no background up to 8,000 km/s. Such "holes" in space are also observed close to other superclusters. A Gaussian curve was fitted to the observed velocity distribution; the resulting mean radial velocity is  $v_0 = 3,399 \pm 39$  km/s and the velocity dispersion is  $\sigma = 684 \pm 38$  km/s which is comparable with the corresponding value for the Virgo cluster.

Further radial velocities of the same quality would not improve the accuracy of the mean radial velocity and the velocity dispersion significantly. But they would be of great help for computations of any three-dimensional dynamical model of this cluster as demonstrated in Fig. 6. As soon as we split up the total sample of radial velocities into subgroups to study the velocity dispersion as a function of distance from the cluster centre, a great number of individual measurements is needed. Owing to the rather small numbers of galaxies in some bins in Fig. 6, an improvement on the observational side is obviously necessary in order to perform smooth modelling. A further strong argument for carrying out observations with the ESO 3.6 m telescope is the fact that in the case of Hydra I, space in front and behind the cluster is quite empty. From the work of Smyth we learn that the Hydra I field still shows strong clustering at an apparent magnitude of  $\sim 17^m.5$ . Thus for this cluster we would be in the unique situation of being able to study the true luminosity function of its galaxies over a range of 6 magnitudes. To be sure of cluster membership this would clearly imply the need for radial velocities observed with the 3.6 m telescope.

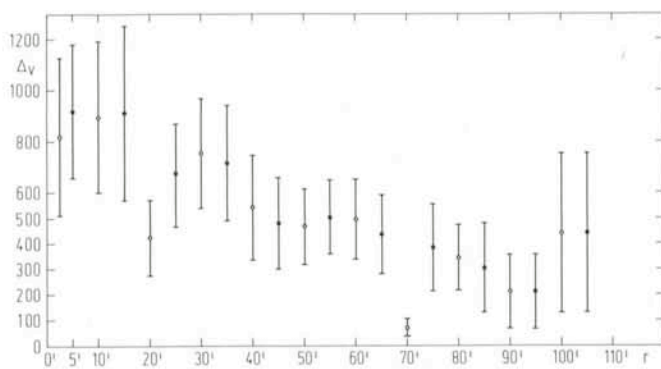


Fig. 6: Velocity dispersion within rings of  $10'$  width around the cluster centre. The data were sampled in two different ways (open and closed circles), where bins were shifted by  $5'$  relatively to each other.

# Structure of the Core of Globular Clusters

Michel Aurière, Pic-du-Midi Observatory

## Introduction

There are numerous astrophysical arguments to stimulate an observer who wishes to study the poorly known central parts of globular clusters. Two considerations are particularly exciting. The theories of dynamical evolution of these stellar systems systematically predict the development of a central singularity; now, if it exists, what is its physical counterpart? In the observational field, we know that at least 15 globular cluster cores are associated with X-ray sources. Such phenomena occur preferentially in concentrated globular clusters. High spatial resolution is needed to disentangle individual stars in the central overcrowded fields. We are currently observing several concentrated globular clusters at Pic-du-Midi Observatory where excellent seeing is not rare. The splendid observations reported at La Silla with the 1.5 m Danish telescope (THE MESSENGER No. 17, p. 14) show that this instrument in its site may be very effective for such research. At any rate, the southern sky is particularly suited for globular cluster studies: it contains more than 100 from the about 140 known galactic globular clusters. Many objects of great interest, as 47 Tuc, the core of which is shown in Fig. 1, are invisible from France.

## The Observational Programme and its Aims:

I have used at the 1.5 m Danish telescope at La Silla the instrumentation especially designed for the globular cluster programme at Pic du Midi. It consists of two interchangeable cameras which are placed behind a focal enlarger adjusted to give a focal length of about 35 m (scale of about 6" per mm). It is known from the experience of planetary observers that a valuable way of securing high spatial resolution images in the case of good seeing is to take a great number of short exposures from which the best ones are selected. The first camera is built around a one-stage image tube. A film holder enables us to take exposures rapidly on 35-mm roll film as with a 35-mm camera. We can obtain in this way unfiltered images of the core of globular clusters with exposure times of a few seconds. These photographs are not suited for photometry but

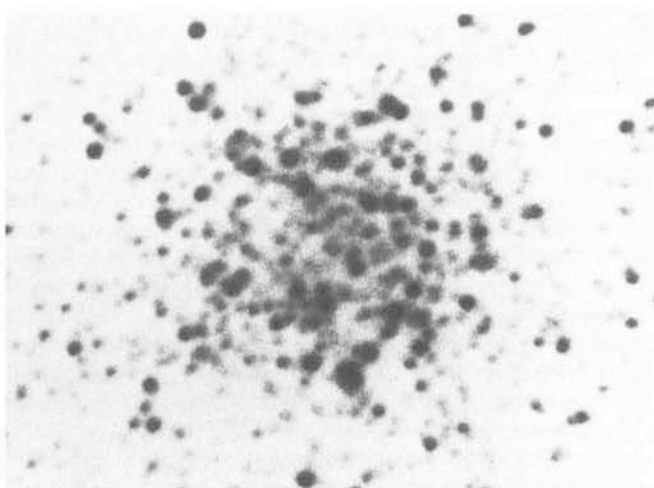


Fig. 1: The concentrated core of 47 Tuc. North: upper right. Field:  $115'' \times 80''$ . 1 sec. unfiltered exposure through the image tube at the 1.5 m Danish telescope.

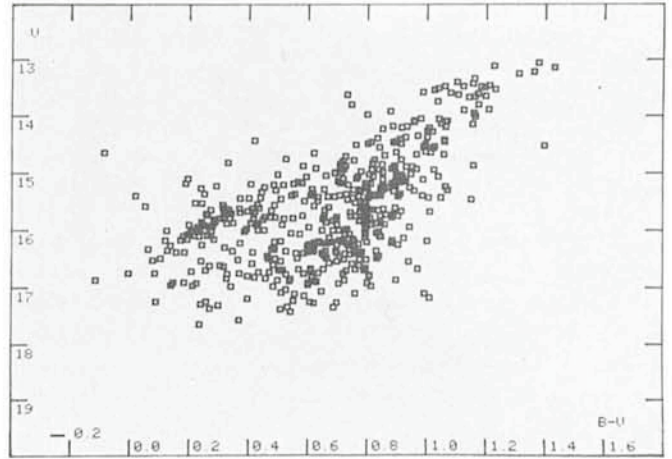


Fig. 2: Colour-magnitude diagram for 505 stars in a  $1' \times 1'$  field centred on the northern X-ray globular cluster M 15.

they give the core structure in stars and make it possible to build a map of the star positions. Photometry is made with photographs taken with a B/V camera including a dichroic glass and filters to record pictures in the two passbands in a single exposure. Again, 35-mm roll film is used. These photographs were calibrated at La Silla with the spot sensitometer in the 3.6 m building. Reduction of this material and astrophysical implications of the data are presented in the proceedings of the ESO/ESA workshop on the Space Telescope (Geneva, February 1979), the first colloquium of the "Comité Français pour le Télescope Spatial" (Toulouse, April 1980) and in several papers in *Astronomy and Astrophysics*. Before presenting the data obtained at La Silla, I give some results from the Pic-du-Midi Observatory study to illustrate what one can expect from such studies. Published results concern mainly M15 (NGC 7078), the only X-ray globular cluster of the northern sky, which has an extremely condensed core and, furthermore, presents a central brightness excess over currently observed profiles (King, 1975, IAU Symposium No. 69, p. 99). One part of our work was to carefully study the central condensation associated with the brightness excess. Its brightest point was found to coincide within  $1''$  with the adopted centre of the cluster: centre of isophotes of faint stars (Leroy et al., 1976, *Astron. Astrophys.*, **53**, 227), equibarycentre of the resolved stars. This is a propitious argument for a theory asking for a massive black hole at the centre of globular clusters, as a consequence of the evolution of the central singularity. This model is able to explain X-ray emission by accretion of gas on the black hole. The brightness of the central condensation in M 15 would be compatible with a black hole of about  $10^3 M_{\odot}$ . Other observations however do not confirm this hypothesis. A search for [O III] emission in the core of M 15 (Aurière et al., 1978) has put an upper limit for the intensity of any point source to 1/70 the brightness of the well-known planetary nebula lying at about  $30''$  from the cluster centre. This result, confirmed by  $H\alpha$  observations (Pic du Midi, unpublished; Philips J. P. et al., 1978, *Astron. Astrophys.*, **70**, 625) infirms previous exciting  $H\alpha$  observations (Peterson A. W., 1976 *Astron. Astrophys.*, **56**, 441; Grindlay et al. *Astrophysical Journal*, 1977, J **216**, L105).

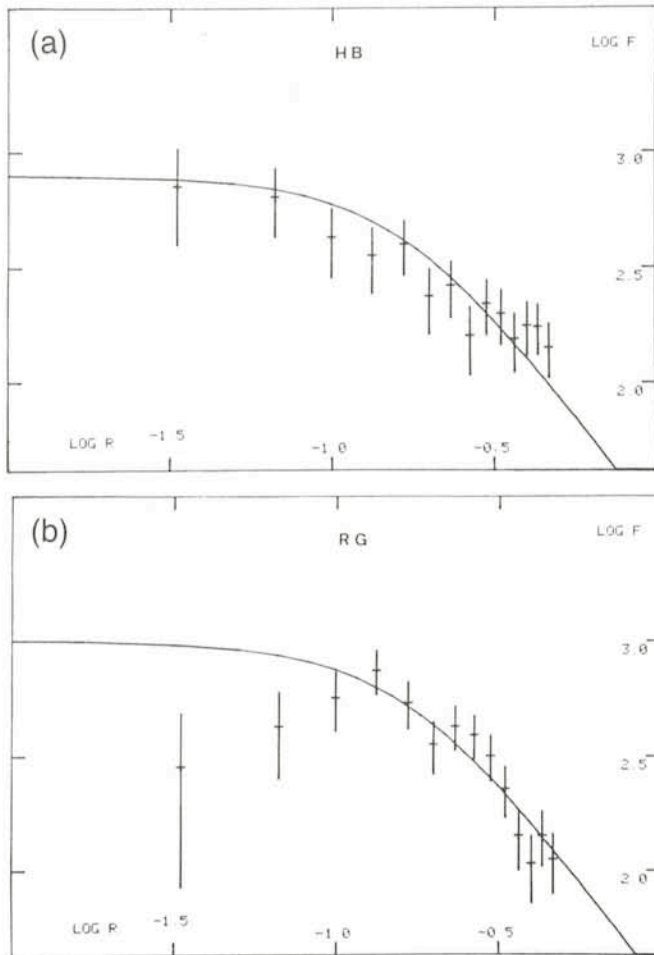


Fig. 3: (a) ( $\log, \log$ ) diagram of the projected density (crosses) for the horizontal branch stars located in the central part of M 15. Crosses are fitted by King's model curves. F: star number by square arcmin. R: distance to cluster in arcmin. (b) Same as (a) for red giants.

Pictures with resolution near  $0.5''$  (taken with the 1 m and 2 m telescopes at Pic-du-Midi Observatory) have enabled us to resolve the central condensation of M 15 into 5 rather faint stellar objects of B-V compatible with common stars of M 15. Spectroscopic observations (Newell B. et al., 1976, *Astrophys. J.*, **208**, L 55; Leroy J.-L., unpublished) confirm that the central condensation in M 15 may not be necessarily composed of exotic objects. As a last observational argument, Einstein X-ray observatory observations have not supported the massive black-hole hypothesis. X-ray sources associated with globular clusters have been found in the cores of these objects but not at their very centre (Grindlay 1980 – Preprint No. 1434 – Center for Astrophysics). In the case of M 15 for which a catalogue of 734 star positions has been obtained (Aurière and Cordoni, 1981, *Astron. Astrophys.* in press) we have been able to locate exactly the X-ray source from Grindlay's position ( $\pm 2''$ ). It falls at about  $6.5''$  from the central condensation in a place without resolved stars. The nearest resolved stars at  $1.5''$  are two close red giants.

Our photometric data concerning the central part of globular clusters were also used to obtain the B and V magnitudes of individual stars. This is done thanks to a special computing procedure described elsewhere. It enables us to plot the colour-magnitude diagram for stars which are spatially different from those which are generally studied. In the case of M 15 (Fig. 2) we were able to confirm the gaps found by Sandage et

## ESO COUNCIL DECISION

At its last meeting on June 4, 1981, the ESO Council has decided that the title of Dr. A. Ardeberg will be changed from "Astronomical director at La Silla" to "Director at La Silla".

al. in the red giant branch (1968, *Astrophys. J.*, **152**, L 129) and to suggest a different slope for this branch. We also used this diagram and the known positions of the corresponding stars to study relative distributions of stars at different stages of evolution and to approach the problem of mass segregation. Dynamical models predict different radial distributions for stars of different masses. Mass loss between red giant and horizontal branches (about 20% of the initial mass) may give an opportunity to observe the phenomenon. However, this would be observable only in clusters where the relaxation time is less than, or of the order of, the life-time on the horizontal branch. If we suppose this life-time to be about  $10^8$  years for the stars involved (Caputo et al., 1978, *Monthly Notices of the Royal Astronomical Society*, **184**, 377), the only objects concerned are the central part of concentrated globular clusters. For example, the central relaxation time of M 15 is about  $10^8$  years, that of NGC 6397 about  $2 \cdot 10^7$  years. Fig. 3 illustrates a problem which is encountered when counting the number of evolving stars in a globular cluster core. Their number is small so that statistical fluctuations may mask a possible mass segregation. To elude this problem, we are gathering data for several comparable clusters and will add them.

## Observations at La Silla

The observing run at La Silla for this programme fell in June 1980. I was not lucky enough to catch excellent seeing in this winter period. The very performant 1.5 m Danish telescope and the adapted instrumentation enabled us to secure several tens of exposures in two nights of effective observation. The spatial resolution of the best short exposures is of about one arc second, which is enough to solve some problems as we will see next. I will present observations made on 3 particular clusters.

The first is 47 Tuc, one of the most famous globular clusters. Fig. 1 shows its core almost completely resolved in its bright stars although it is very concentrated. Fig. 1 is a good complement to classical images showing the whole object but with the central part completely unresolved. The run was only exploratory for this object which was observed far from the meridian. This young cluster (about  $10^{10}$  years) is rather close (at about 5 kpc); it is puzzling because it presents a well-established radial colour variation. Furthermore, from Grindlay's observations with the Einstein Observatory, its core is known to be associated with an X-ray source. We hope that our observations will explain the radial colour variations (in term of variations of the luminosity function of the red giant branch?)

NGC 6397 was one of the main targets of the run: it is one of the two nearest globular clusters, at 2.4 kpc, that is four times nearer than the classical M 3, M 15 . . . famous in the northern sky. This means that observations with  $0.5''$  seeing, already encountered at La Silla, would place one in a position very near to observing M 3, M 15 . . . with the Space Telescope! Moreover, NGC 6397 has two very important characteristics from the dynamical point of view: it is very old ( $17 \cdot 10^9$  years according to Alcaïno and Liller, in *Star Cluster*, IAU Symposium No. 85, p. 423) and its central relaxation time is small ( $2 \cdot 10^7$  years). So

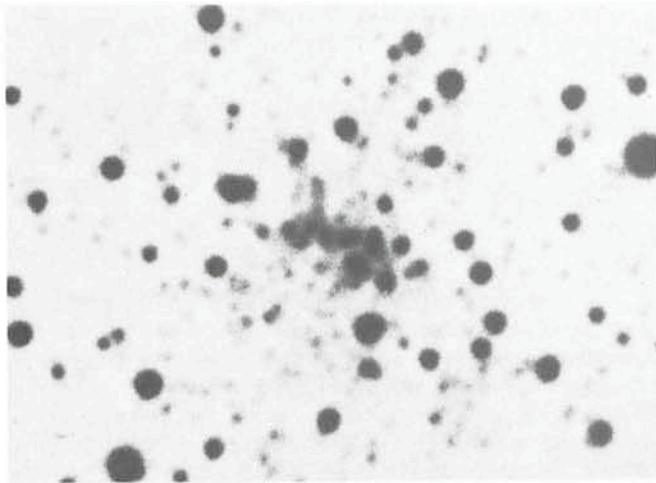


Fig. 4: The core of NGC 6397 and its central condensation. North: upper right. Field:  $85'' \times 60''$ . 8 sec unfiltered exposure through the image tube at the 1.5 m Danish telescope.

it is dynamically very advanced and it is a very good case for a possible central singularity. The  $1''$  resolution photographs of NGC 6397 secured at La Silla are twice as resolvable in parsec as the best ones obtained for M 3 and M 15. In the very centre of the cluster (Fig. 4) we see a condensation of rather faint stars. Radial brightness profiles obtained from the B and V images show that this feature induces a central luminous excess above the isothermal profile. The size of the central condensation is about  $10''$  or 0.1 pc, which is very near to that of M 15. NGC 6397 seems to be a case of a globular cluster showing a central condensation of rather faint stars. The works of Illingworth and King (1977, *Astrophys. J.*, **218**, L 109) and Heggie (1979, IAU Symposium No. 85), for example, have shown that such central condensations can be explained as the result of collapsed cores. The observational study of these condensations needs high spatial resolution to rule out possible effects of random clumping of bright stars.

M 30 (NGC 7099) was also observed at La Silla. Its declination (about  $-23^\circ$ ) permits observations from Pic du Midi. It is

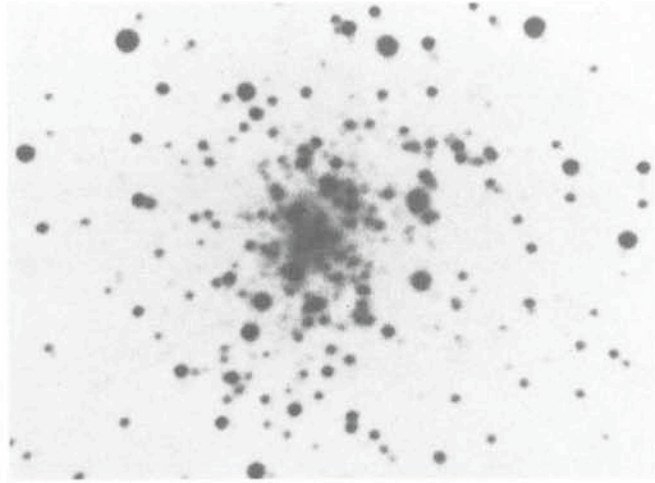


Fig. 5: The central part of the very condensed core NGC 7099 (M 30). North: upper left. Field  $100'' \times 70''$ . 5 sec unfiltered exposure through the image tube at the 1.5 m Danish telescope.

an example of object that can be observed from the two observatories. Fig. 5 shows one of the short exposures obtained at La Silla which will enable us to work on the B and V photographs obtained from La Silla as well as from Pic du Midi. M 30 is very concentrated and has a central relaxation time of only  $1.5 \cdot 10^7$  years. Its core is rather poor in bright stars. We will check if the deficiency in red giants observed in the outer parts is also present in the central part.

### Conclusion

A first exploratory observing run at La Silla for studying the core of globular clusters has been fruitful. We have obtained new results and demonstrated that the site is well suited for such research. We plan to have new observations to try to reach still better spatial resolution and to investigate other objects. The investigation will also be extended to Magellanic Cloud globular clusters. If we astutely choose our targets, we might be able to tackle problems which are often believed to be reserved to the Space Telescope.

## Visiting Astronomers

(October 1, 1981 – April 1, 1982)

Observing time has now been allocated for period 28 (October 1, 1981 – April 1, 1982). As usual, the demand for telescope time was much greater than the time actually available.

The following list gives the names of the visiting astronomers, by telescope and in chronological order. The complete list, with dates, equipment and programme titles, is available from ESO-Garching.

### 3.6 m Telescope

Oct. 1981: Azzopardi/Breysacher/Lequeux/Maeder/Westerlund, Véron, M. P. and P., Wlérick/Cayatte/Bouchet, Westerlund, de Graauw/Israel/van de Stadt/Habing, van Dessel/van Paradijs/Burger/de Loore, Seitter/Teuber, Melnick/Terlevich/McMahon, de Ruiten/Zuiderwijk, Pizzichini/Danziger/Grosbøl/Pedersen, Tarengi, Rosa/D'Odorico, D'Odorico/Baade.

Nov. 1981: D'Odorico/Baade, Hunger/Kudritzki/Simon, D'Odorico/Moorwood, Moorwood/Salinari, Moorwood/Shaver/Salinari, Dennefeld, Thé/Alcaino, Grewing/Schulz-Lüpertz, Wehinger/Gehren/Wyckoff, Macchetto/Perryman/di S. Alighieri, Marano/Braccisi/Zitelli/Zamorani, Valentijn, Wlérick/Cayatte/Bouchet.

Dec. 1981: Wlérick/Cayatte/Bouchet, Lindblad/Athanassoula/Grosbøl/Jörsäter, Grosbøl, Wilson/Ziebell, Rouan, Braz/Lepine/Epchein, Nguyen-Q-Rieu/Epchein, Epchein/Nguyen-Q-Rieu/Braz, Papoular/Epchein/Le Bertre, Fricke/Kollatschny/Schleicher/Witzel, Schnur, de Ruiten/Lub, Giuricin/Hazard/Mardirossian/Mezzetti/Terlevich, Nelles/Richtler, Miley/Heckman.

Jan. 1982: Miley/Heckman, Pettersson, Thé/Koornneef, Olofsson/Nordh/Fridlund/Koornneef, Eichendorf/Krautter, Krautter/Eichendorf, Eichendorf/Reipurth, van Dessel/van Paradijs/Burger/de Loore, Eichendorf/Reipurth, Danziger/de Ruiten/Kunth/Lub/Griffith, Gahm/Krautter, Mouchet/Motch/Ilovaisky/Chevalier.

- Feb. 1982: Mouchet/Motch/Ilovaisky/Chevalier, Lamy/Koutchmy, Chevalier/Ilovaisky/Fauconnier/Dreux/Fort/Motch/Hurley, Fort/Vigroux/Kunth, Reimers/Koester, Koester/Weidemann.
- March 1982: Koester/Weidemann, Kollatschny/Fricke/Collin-Souffrin/Dumont, Engels, Combes/Encrenaz/Zeau/Berezné/Arfouillaud, Kudritzki/Simon/Méndez, Audouze/Dennefeld, Cetty-Véron, Tarengi, Ardeberg/Lindgren/Nissen.

### 1.5 m Spectrographic Telescope

- Oct. 1981: Ferlet/Maurice/Prévot, Duerbeck, Maurice/Waelkens, Spite, F. and M./Barbuy, D'Odorico/Baade, Vidal, Boisson.
- Nov. 1981: Boisson, Muratorio, Maurice/Waelkens, Grewing/Schulz-Lüpertz, Louise, Grosbøl, Maceroni/Milano/Russo/Nesci.
- Dec. 1981: Maceroni/Milano/Russo/Nesci, Finkenzeller, Baade, Drechsel/Wargau/Rahe, Wamsteker/Danks, Pettersson, Krautter/Reipurth.
- Jan. 1982: Krautter/Reipurth, de Loore/van den Heuvel/van Paradijs, Stahl/Wolf, Eichendorf/Nieto, Eichendorf/Reipurth, Appenzeller/Marenbach, Rucinski, Andriillat.
- Feb. 1982: Andriillat, Vreux, Holweger, West/Barbon/Capaccioli, Fricke/Kollatschny/Schallwich/Schleicher/Yorke, Ilovaisky/Chevalier.
- March 1982: Ilovaisky/Chevalier, Dachs, Gehren, Ardeberg/Maurice, Véron, P., Bertola/Galletta, Darius/Barbier.

### 1.4 m CAT Telescope

- Dec. 1981: Andersen/Gustafsson/Lambert.
- Jan. 1982: Andersen/Gustafsson/Lambert, Habing/Burton/de Graauw/Israel/van de Stadt, Gerbaldi, Paraggiana/Floquet/van Santvoort.
- Feb. 1982: Gerbaldi/Paraggiana/Floquet/van Santvoort, Holweger, Ferlet/Bruston/Audouze/Laurent/Vidal-Madjar, Ferlet/Dennefeld, Ferlet/York, Dravins/Lind.
- March 1982: Dravins/Lind, Nissen, Frisk/Olofsson.

### 1 m Photometric Telescope

- Oct. 1981: Westerlund, Westerlund/Lundgren, Ferlet/Maurice/Prévot, Breysacher/Perrier, Melnick/Terlovich, Beck/Wielebinski/Schnur.
- Nov. 1981: Beck/Wielebinski/Schnur, Moorwood/Shaver/Salinari, Vanbeveren, Grewing/Schulz-Lüpertz, Thé/Alcaïno, Bues/Rupprecht.
- Dec. 1981: Bues/Rupprecht, Marano/Braccesi/Zitelli/Zamorani, Epchtein/Nguyen-Q-Rieu/Braz, Nguyen-Q-Rieu/Epchtein, Papoular/Epchtein/Le Bertre, Fridlund/Nordh/Olofsson, Alcaïno, Richtler/Nelles, Pettersson, Wlérick/Cayatte/Bouchet.
- Jan. 1982: Wlérick/Cayatte/Bouchet, Terzan, Reipurth, Geyer/Richtler, van Woerden/Danks.
- Feb. 1982: van Woerden/Danks, Kohoutek, Schneider/Maitzen, Bastien/Bertout, Mattila/Schallwich/Fricke/Schnur.
- March 1982: Mattila/Schallwich/Fricke/Schnur, Dachs, Engels, Gammelgaard/Kristensen, van Woerden/Danks, Cetty-Véron.

### 50 cm ESO Photometric Telescope

- Oct. 1981: Thé/Alcaïno, Gyldenkerne/Hawkins.
- Nov. 1981: Gyldenkerne/Hawkins, Schneider/Maitzen, Caplan/Deharveng/Sivan.
- Dec. 1981: Caplan/Deharveng/Sivan, Schoembs, Isaak, Wolf/Stahl/Sterken.
- Jan. 1982: Wolf/Stahl/Sterken, Rucinski, Kohoutek, Thé/Karman.
- Feb. 1982: Thé/Karman, Bastien/Bertout, Mattila/Schallwich/Fricke/Schnur.
- March 1982: Mattila/Schallwich/Fricke/Schnur, Mauder, Debehogne, Lagerkvist/Rickman, Schober.

### GPO 40 cm Astrograph

- Oct. 1981: Azzopardi.
- Nov. 1981: Schmidt-Kaler/Tüg, Bijaoui/Lacoarret/Le Van Suu.
- Dec. 1981: Bijaoui/Lacoarret/Le Van Suu.
- Jan. 1982: Burnage.
- March 1982: Debehogne/Vieira Gilson.

### 1.5 m Danish Telescope

- Oct. 1981: Ardeberg, Maurice.
- Nov. 1981: Crane/Motch/West/Kruszewski, Crane, Motch/Ilovaisky/Chevalier/Crane/Hurley, Kruszewski/West.
- Dec. 1981: Kruszewski/West, van Paradijs/van der Klis, Lyngå, Imbert/Prévot.
- Jan. 1982: Imbert/Prévot, Andersen/Nordström, Sol, Lortet/Testor/Heydari-Malayeri/Pedersen/Lub, Mouchet/Motch/Ilovaisky/Chevalier.
- Feb. 1982: Mouchet/Motch/Ilovaisky/Chevalier, Lortet/Testor/Heydari-Malayeri/Pedersen/Lub, Ardeberg.
- March 1982: Tarengi.

### 50 cm Danish Telescope

- Oct. 1981: Sterken/Jerzykiewicz, Rucinski.
- Nov. 1981: Rucinski, Schneider/Maitzen.
- Dec. 1981: Baade, Lyngå.
- Jan. 1982: Lyngå, Renson/Manfroid.
- Feb. 1982: Clausen.
- March 1982: Clausen.

### 90 cm Dutch Telescope

- Oct. 1981: Maurice/Lub.
- Nov. 1981: Pel, de Ruiter/Lub.
- Dec. 1981: de Ruiter/Lub.
- Jan. 1982: Krautter/Reipurth, Seggewiss, Darius/Barbier.
- Feb. 1982: Darius/Barbier.
- March 1982: Cuyppers, Gathier/Pottasch.

# Non-Atlas Photographic Work in the Sky Atlas Laboratory

*Claus Madsen, ESO*

As is well known to the readers of the MESSENGER, the ESO Sky Atlas Laboratory was established to set up and undertake the production of the ESO/SRC Sky surveys. To fulfil its duties, a number of dark rooms were set up and, after some years of hard work, techniques were developed which permit limited mass-production without sacrificing the quality which has become the hallmark of this project.

Apart from its major task, a number of other jobs are executed in the Sky Atlas Laboratory, ranging from the production of publicity photos to special black-and-white work directly related to astronomy. Furthermore, the installation of colour-printing facilities was envisaged by the planners of the new

ESO headquarters in Garching. The colour laboratory is about to commence operations (pending final installation).

One major problem in reproducing spectroscopic plates is caused by the enormous density range of the original plates. Whereas this has been solved in a satisfactory way in connection with the copying of the Atlas, the same solution cannot be applied when prints have to be made, due to the fact that photographic paper is unable to cover the density range of the original (or copy) plate. The b/w work therefore includes the application of special contrast manipulation techniques, such as masking, which have proved to be very efficient in bringing out very fine details, especially in heavily exposed parts of the

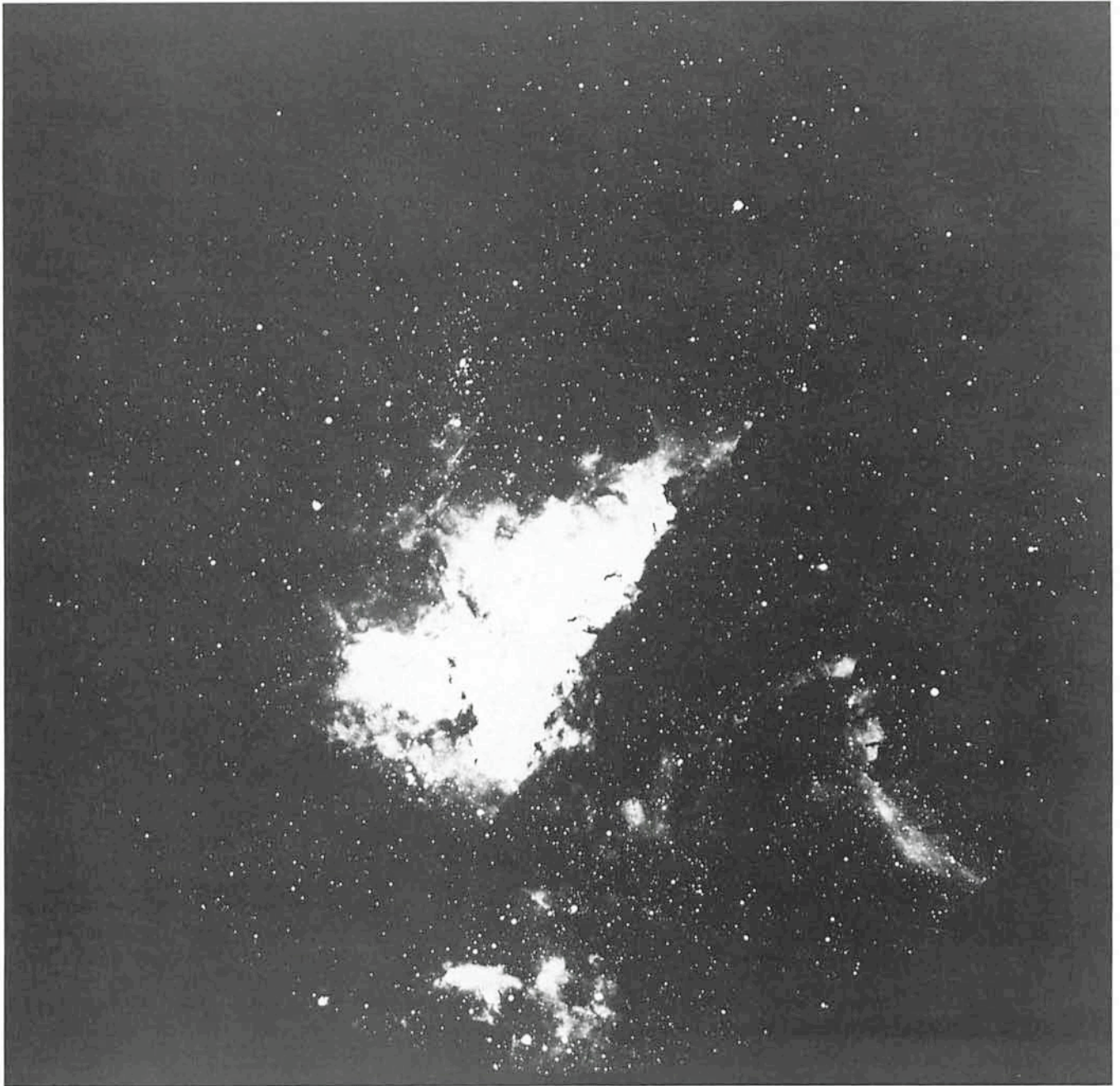


Fig. 1: This photograph of Eta Carinae was obtained by ESO astronomer Massimo Tarenghi with the 3.6 m telescope. The density range of the plate is  $\Delta D = 2.68$  which by far exceeds the dynamic range of the printing paper.

plates (e.g. nebulae). Due to the very limited density range of the paper, it is virtually impossible to retain such details by normal printing (Fig. 1). The introduction of a low-contrast photographic mask in the printing phase, however, ensures a much better reproduction (Fig. 2). It goes without saying that using such a mask requires a great deal of accurate work on the part of the photographer in order to obtain a sharp picture, since it must be kept in perfect registration with the original or the printing paper during the process.

Other tasks include contrast enhancement, e.g. to show the extension of very faint galaxies (Fig. 3), the production of pictures with diagrammatic overlays, etc.

A lot of interest focuses on the colour laboratory currently being set up. The lab itself centres around an Italian-made Durst Repro-Laborator 1800 enlarger, fitted with a colour head featuring dichroic filters with a range of 195 CC values (used to influence the colour balance of the prints).

There is a German-made Autopan 60–40 C processing machine intended for the Ciba P–3 colour process. Control is achieved by means of Macbeth transmission and reflection densitometers.

Unlike the more common colour processes (based on the chromogenic development), the Ciba one is based on the bleaching of excess colour dyes in the emulsion in order to produce a picture of proper density and colour balance. The presence of the colour dyes in the emulsion during the exposure very drastically reduces the scattering of light in and between the emulsion layers, permitting a sharpness hitherto unknown with common colour materials. Furthermore, the stability of the colour dyes has been proved to exceed by far that of the dyes formed in chromogenic development. The process stability is generally regarded as good, ensuring a homogenous quality even when the output is relatively small as it may be at certain times of the year. Finally, the self-masking



Fig. 2: A masked print of the same plate shows a vast increase in details.

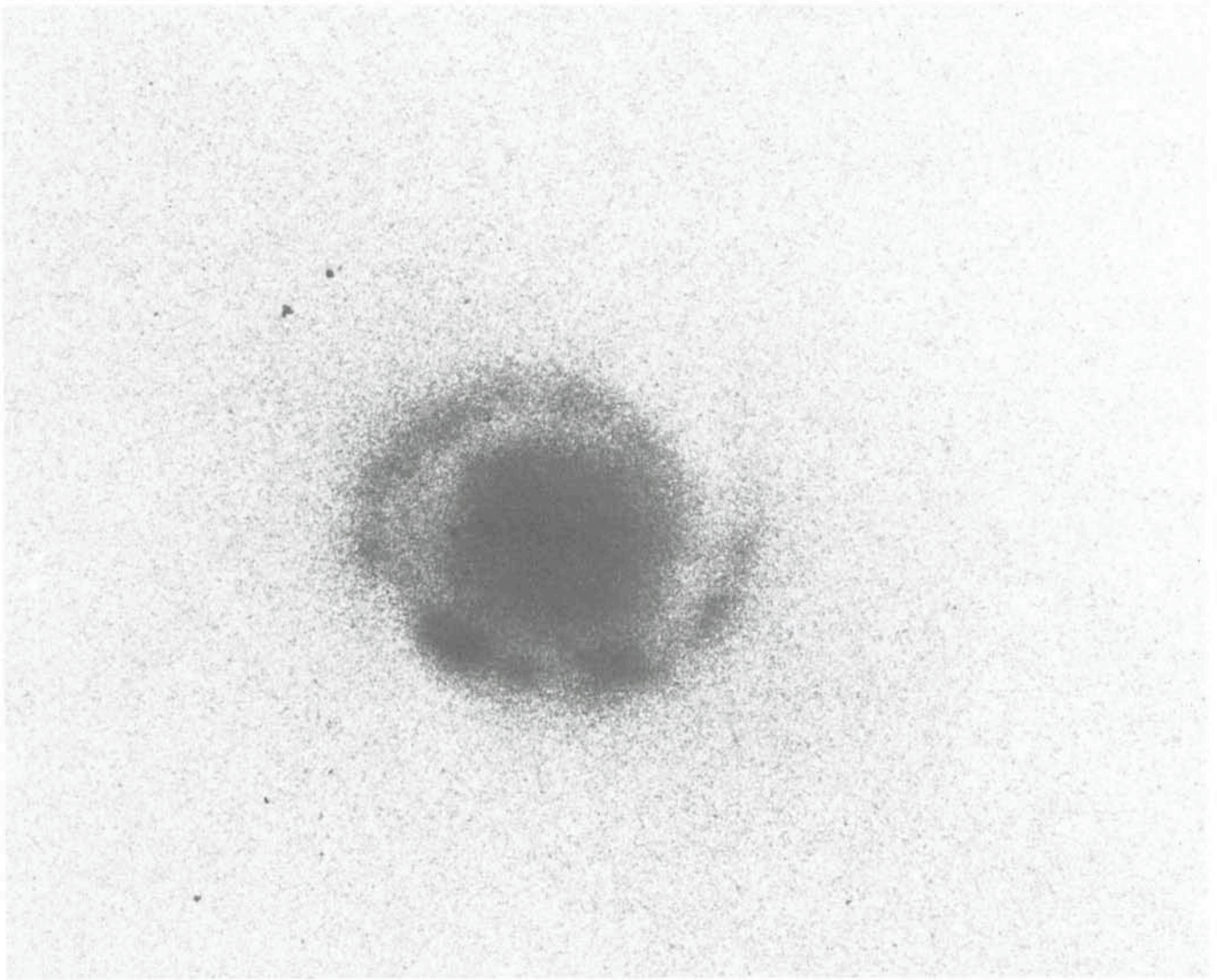


Fig. 3: Contrast manipulation can be a matter of contrast enhancement, too, like this photograph of NGC 1510, which was originally made on a IIIa-J plate. An intermediate film copy was made featuring a greatly increased contrast.

P-3 process offers a significant improvement in colour rendition as compared to the Cibachrome-A process which is being used elsewhere.

Trial runs with the machine have already been made and (at the time of writing) we are awaiting the final details of installation.

The colour laboratory will enable us to produce colour prints and large colour transparencies from colour slides (or b/w colour separation film). In order to use the lab properly for reproducing astronomical materials, the original transparencies will have to be of good quality. As is well known, rather poor results are obtained if ordinary colour film is used at the telescope. Two major obstacles are generally held responsible for this fact: the bad performance of the film when it is subjected to excessive exposure times (the Low Intensity Reciprocity Failure) and lack of spectral sensitivity. As far as LIRF is concerned, the techniques normally used to overcome these problems in the black-and-white film cannot be applied because the three main layers of the colour material respond differently to low-intensity exposures (very often resulting in a "crossed-curves" condition), producing a noticeable colour cast which unfortunately cannot be corrected. Attempts to

overcome the LIRF problem by means of cooling the emulsion have been quite successful, and fairly good results have been obtained in this way. However, the cooling of large colour films at the telescopes appears to be very difficult from a technical point of view. Consequently much attention has been paid to alternative ways of colour printing. One method, which forms the basis of our project, involves the revival of the old additive printing technique (three-colour printing). It is our intention to make prints by means of superpositioning b/w plates (of the same object, but exposed in different pass bands) and exposing them sequentially onto colour duplicating film or colour printing paper through filters of the three additive primary colours. Apart from bypassing the above-mentioned problems, this method has the obvious advantage that existing plates can also be used. The major difficulties are the alignment of the plates (inaccuracy leads to three different images in the primary colours of each object) and adjusting the contrast in order to ensure a printable density range as well as a proper colour balance. In the coming months, much time will have to be devoted to these problems, but once we have found their solutions, we expect to be able to produce colour prints of interest not only to the public but also, of course, to the astronomical community.

# Do T Tauri Stars Have Extensive Coronae?

Joachim Krautter, ESO, and Gösta Gahm, Stockholm Observatory

## Introduction

T Tauri stars are low-mass ( $\leq 3 M_{\odot}$ ) pre-main-sequence stars. They have been recognized the first time as an individual group of stars in 1945 by Alfred Joy. They show irregular photometric variability and are located without exception, or very close to, dark clouds. In 1958 another pioneer of variable-star research, George Herbig, proposed a number of spectroscopic criteria:

(1) The hydrogen lines and the H and K line of Ca II are in emission.

(2) The fluorescent Fe I emission lines  $\lambda\lambda$  4063, 4132 are present.

(3) Forbidden lines are often present.

(4) In those stars which show an absorption spectrum (from late F to M) Li I  $\lambda$  6707 is present as a strong absorption line. Later, more characteristics have been found for T Tauri stars, e. g. IR excess, "veiling", complex emission line profiles and a lot more. The strength of the emission lines varies strongly from star to star. In the following we want to discuss some emission-line properties and the place of their origin.

Already Joy mentioned that the spectrum of T Tauri stars resembles the chromospheric spectrum of the sun, the so-called "flash" spectrum. In this spectrum, which originates in the solar chromosphere, all the Fraunhofer lines of the photospheric absorption spectrum are seen in emission. But the chromospheric spectrum is in no way a simple reversion of the photospheric spectrum, since the strength of lines of ionized atoms and of highly excited atoms is enhanced compared to the absorption line strength. The strongest lines in the flash spectrum are the Ca II H and K lines, the hydrogen lines of the Balmer series and the He I  $\lambda\lambda$  4471, 5876 lines. Since the Balmer lines and the Ca II H and K lines are normally the strongest emission lines in the spectrum of a T Tauri star (see Herbig's criterium (1) and He I is often present in emission, one immediately recognizes the similarity. Herbig suggested in 1970 that the same mechanism producing the solar chromosphere is also operating actively in T Tauri stars.

## UV and X-ray Observations of T Tauri Stars

Observations of T Tauri stars in the satellite UV spectral range with the International Ultraviolet Explorer (IUE) provided us with new information on the emission line chromospheric region. As an example Figure 1 shows the UV spectra ( $1200 \text{ \AA} \leq \lambda \leq 3200 \text{ \AA}$ ) of the T Tauri stars DR Tau, CoD - 35° 10525 and AS 205 observed by Appenzeller et al. (*Astronomy and Astrophysics*, **90**, 184, 1980). Common to all spectrograms is the occurrence in emission of certain strong resonance multiplet and ground-state intercombination lines such as Mg II, Si II, Si III, Si IV, C I, C III, C IV, etc. Also a number of emission lines of singly ionized metals are present. As shown by the figure, the relative strength of the emission lines and the line emission strength relative to the continuum varies from star to star. (One should note, however, that in Figure 1 the wavelength positions of various expected spectral lines or blends are indicated. Therefore, not all indicated features are regarded by the authors as real.)

These emission lines reveal the presence of very hot regions around the stars. The ion of highest ionization stage observed is the N V  $\lambda$  1238 resonance doublet. This line, present in DR Tau and in CoD -35° 10525 (and in RU Lup), requires some

200,000 K to be formed. Hence the emitting regions around T Tauri stars cover a large range in temperature – from about 7,000 K to at least 200,000 K! (For further interpretation of the UV spectra we refer the reader to the review article by G. Gahm in "The Universe in Ultraviolet Wavelengths: The First Two Years of IUE", ed. R. D. Chapman, NASA publication).

A quantitative analysis of the emission line spectrum can be done by calculating volume emission line measures  $Vn_e^2$ . This quantity is a characteristic measure of the emissivity of an envelope. The volume emission line measures that can be derived from emission lines formed at different temperatures can be  $10^4$  to  $10^6$  larger than the corresponding solar values (Cram et al., *Astrophysical Journal*, **238**, 905, 1980; Gahm in the above cited review article). For a given star this scaling factor is approximately the same for lines found at different temperatures. In other words: Chromospheres of T Tauri stars are ten thousand to one million times more "powerful" than the solar chromosphere!

At this point arises of course our title-question: Do T Tauri stars also have such powerful  $10^6$  K coronae with scaling factors up to  $10^6$  compared to the solar corona? Indeed, recently such coronae with temperatures between one and two

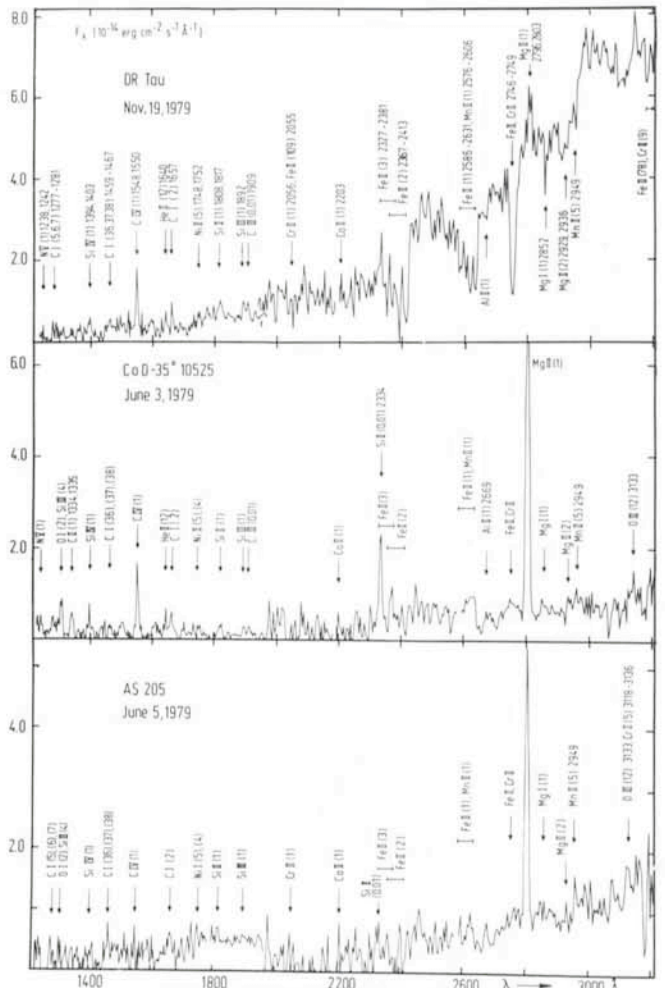


Fig. 1: UV spectrograms of the T Tauri stars DR Tau, CoD - 35° 10525, and AS 205 (from Appenzeller et al., *Astron. Astrophys.*, **90**, 184, 1980).

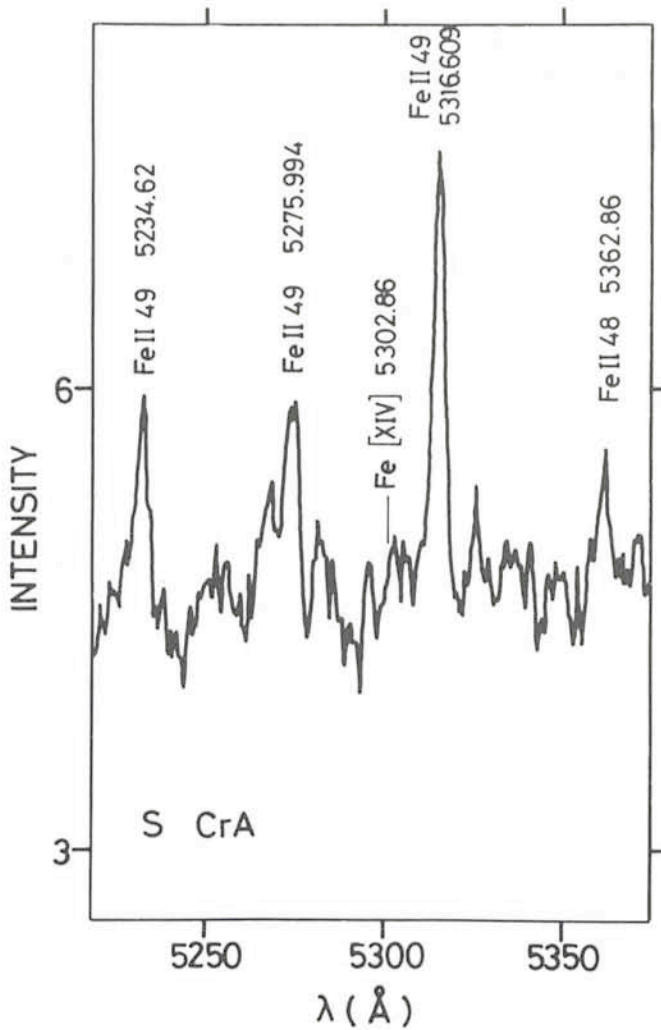


Fig. 2: Spectral region around the  $[Fe\ XIV]\ \lambda\ 5303$  line in S CrA.

million Kelvin have been proposed in theoretical models by various authors. These models predict strong X-ray radiation from such  $10^6$  K coronae.

An excellent way to check this prediction are X-ray surveys with the Einstein observatory. Several surveys have been carried out by Gahm (*Astrophys. J.*, **242**, L163, 1980), Feigelson and de Campi (*Astrophys. J.*, **243**, L89, 1980), and Walter and Kuhi (preprint). But for most T Tauri stars no X-ray flux could be detected. Furthermore, with one exception, all T Tauri stars detected with Einstein show only very weak emission lines in the visual spectral range. The X-ray luminosities of these stars are up to  $10^5$  times larger than the corresponding solar values. For most stars with strong emission lines like RU Lup, RW Aur, and S CrA no X-rays were detected at all. When comparing with the X-ray flux from the sun in the same energy band, the corresponding scaling factor is less than 1,000.

One explanation for this behaviour is that T Tauri stars have coronae which are  $10^4$  to  $10^6$  times as strong as the solar corona, but most X-rays are absorbed in circumstellar gas which does not contribute to the visual extinction towards the star. Some stars, especially those with weak emission lines, have only little circumstellar gas and appear as strong X-ray sources.

But there is another possible explanation: Those T Tauri stars which were not detected at X-ray energies do not have powerful  $10^6$  K coronae. The X-ray activity observed could

be explained by some flare-like activity. This assumption is strengthened by the extremely rapid variations which have been found in the X-ray flux of DG Tau, the T Tauri star with the strongest emission lines in the visual spectral range.

### Coronal Line Emission of T Tauri Stars

We have seen that X-ray observations cannot unambiguously clarify our title question. But fortunately observations in the visual spectral range can help us. From spectroscopic observations of the solar corona we know that there are two strong coronal emission lines in the visual spectral range, namely the "green" coronal line of forbidden  $[Fe\ XIV]\ \lambda\ 5303$  and the "red" coronal line of forbidden  $[Fe\ X]\ \lambda\ 6375$ . These lines are formed at temperatures of about  $10^6$  K.

The idea is now: If we find such a coronal emission line in the spectrum of a T Tauri star we can compare the absolute flux of this line with the flux of the corresponding solar line. By doing so we again obtain a scaling factor for the corona of the T Tauri star compared to that of the sun. If we do not find coronal lines in the spectra of T Tauri stars we can at least give an upper limit for the line flux and hence for the scaling factor. A first attempt was made by Gahm et al. (*Monthly Notices of the Royal Astronomical Society*, **195**, 59 p, 1981) who found for RU Lup from the  $[Fe\ X]\ \lambda\ 6375$  line an upper limit for the scaling factor of 6,000.

In our programme, red spectrograms of a sample of 14 T Tauri stars were carefully searched by us for coronal line emission. The spectrograms of 11 stars were obtained with the Boller and Chivens spectrograph at the Cassegrain focus of the ESO 1.5 m telescope. The spectrograms were recorded on Ila-O plates behind a 2-stage Carnegie image tube. Calibration plates were taken with the spot sensitometer. The spectrograms of the remaining 3 T Tauri stars were obtained with the B&C spectrograph in the Nasmyth focus of the 1.23 m telescope of the Calar Alto observatory, Spain. For these observations an electrostatically focused single stage ITT F4078 intensifier and 103a-D plates were used.

The result of our search was that none of our spectra showed any of the coronal lines in emission. As an example Figure 2 shows the spectral region around the  $[Fe\ XIV]\ \lambda\ 5303$  line of the T Tauri star S CrA. Identifications for the most prominent emission lines are given. The position of the  $[Fe\ XIV]$  line is indicated by a dash. Due to the total absence of any coronal emission line we could determine only upper limits for the fluxes of the lines.

This procedure shall be described in short: At first we set an upper limit for the equivalent width of the coronal line. For that we determined the noise level and assumed a maximum line width of the coronal line. Since in a number of T Tauri stars the width of the emission lines decreases with increasing degree of ionization we expect possible coronal lines to be relatively narrow.

With this upper limit of the equivalent width, the continuum flux at the corresponding wavelength, the distance of the star, and the interstellar absorption, we could calculate upper limits for the absolute fluxes of the coronal lines.

In reality there have been some difficulties: Since simultaneous photometric observations existed only for two stars, average photometric values had to be used for most of our stars. In addition, the interstellar absorption is not known for many stars; we have adopted an  $A_V = 1.5$ , a value relatively high for a T Tauri star. There are also uncertainties in the distances of the stars. But since these uncertainties can affect our results in both directions we think that we got good average values.

By comparison with the absolute fluxes of the solar coronal lines which were measured when the sun was in a quiescent state we got the result that for 10 stars the upper limit of the scaling factors are between 2,000 and 8,000. We have got higher values for the other 4 stars because we have spectroscopic data only for the  $\lambda$  6375 line, the intensity of which in the sun is smaller by a factor of 4.5 compared to the  $\lambda$  5303 line. Since these results are for the quiet sun, we would get even lower values if we took the absolute solar line fluxes for a more active sun.

These results lead us to the conclusion that the intensity of any  $10^6$  K corona is less than 8,000 times that of the sun, while lines forming in  $10^4$  to  $10^5$  K gas are  $10^4$  to  $10^6$  times stronger than those of the sun. From this one may conclude that T Tauri stars in general do not have an extensive corona.

## Proceedings of the ESO Conference on “Scientific Importance of High Angular Resolution at Infrared and Optical Wavelengths” Now Available

The proceedings of this conference have just been published. The price for the 450-page volume is DM 50,- (including postage) and has to be prepaid.

Please send your order to:

European Southern Observatory  
Karl-Schwarzschild-Str. 2  
D-8046 Garching bei München  
Fed. Rep. of Germany

# Paschen and Balmer Lines in Active Galactic Nuclei

*K. J. Fricke and W. Kollatschny, Universitäts-Sternwarte Göttingen*

## 1. Introduction

If there is substantial disagreement between an observational result and its expectation from established theory, astronomers tend to speak of a “problem”. One of those problems which bothered optical and UV astronomers during the past years is the discrepancy of the observed ratio of the Ly $\alpha$  and H $\beta$  line intensities with the value of this ratio predicted by simple recombination theory for a photoionized hydrogen gas.

In this process, ionization electrons are recaptured into higher levels and excited atoms formed this way decay to successively lower levels by radiative transitions, finally reaching the ground level. Thereby the various hydrogen recombination spectra are emitted. The lowest of them are the Lyman, Balmer and Paschen spectra (cf. Fig. 1). Now, the Ly $\alpha$ /H $\beta$  ratio observed in quasars and active galactic nuclei are found to be by a factor of 3 to 10 times less than the theoretically predicted value ( $\sim 30$ ). There may be ways around the Ly $\alpha$ /H $\beta$  problem by modifying the simple theory, but the solutions are unfortunately not unique. Some theorists believe that special radiative transport effects in the spectral lines and electron collisions during the line-formation process cause enhanced Balmer line strengths and thereby depress the Ly $\alpha$ /H $\beta$  ratio. If the entire discrepancy is not to be explained by such processes alone, interstellar dust within and/or around the line-emitting regions (which are up to several light years across) may help to reconcile theory with observations (cf. e.g. Davidson, K. and Netzer, H., 1979, *Rev. Mod. Phys.*, Vol. 51, No. 4, p. 715). To explain this, we have plotted in Fig. 2 the standard interstellar extinction curve as a function of wavelength known from our Galaxy. Along the curve we indicated the locations of the various hydrogen lines. It is obvious that the influence of dust extinction on these lines must be quite different due to its strong wavelength dependence. It is also recognized that P $\alpha$  and P $\beta$  are relatively unaffected by dust as a result of the decrease (approximately  $\propto 1/\lambda$ ) of the extinction curve towards longer wavelengths. Moreover, because P $\alpha$  and H $\beta$  originate from the same upper atomic level, the P $\alpha$ /H $\beta$  ratio may be used as a sensitive indicator for the existence and importance of reddening by dust in addition to, or instead of, Balmer line enhancement due to optical depth effects. Therefore the measurement of the near infrared P $\alpha$  and P $\beta$  lines at 1.88 and 1.28  $\mu$ m,

respectively, may help to pin down an appropriate theoretical model for the hydrogen-emission-line region.

## 2. IR Spectrophotometry of P $\alpha$

As a result of strong efforts at various places (Caltech, ESO, La Jolla) on the technical side, the sensitivity and spectral resolution of infrared detectors has been substantially improv-

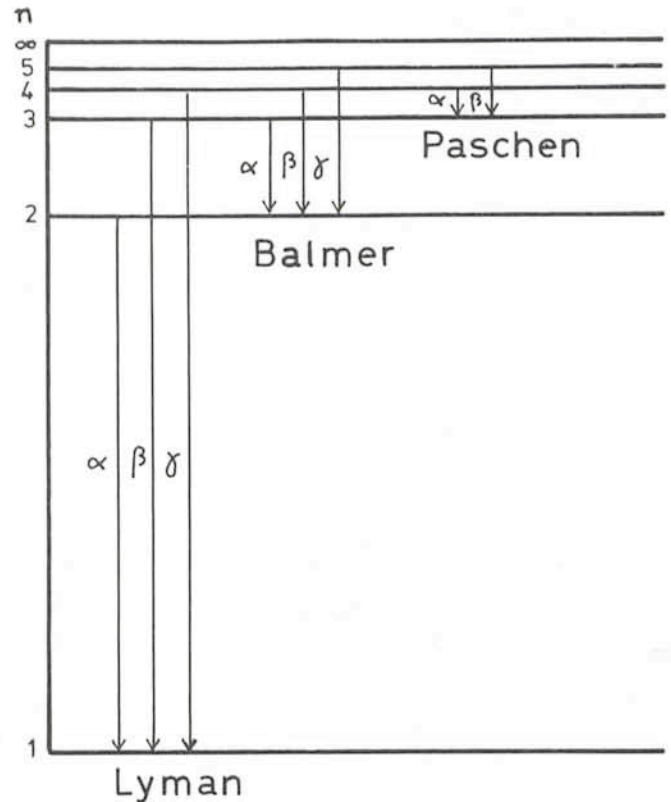


Fig. 1: Energy-level diagram for the hydrogen atom showing the Lyman, Balmer and Paschen series.  $n$  is the principal quantum number.

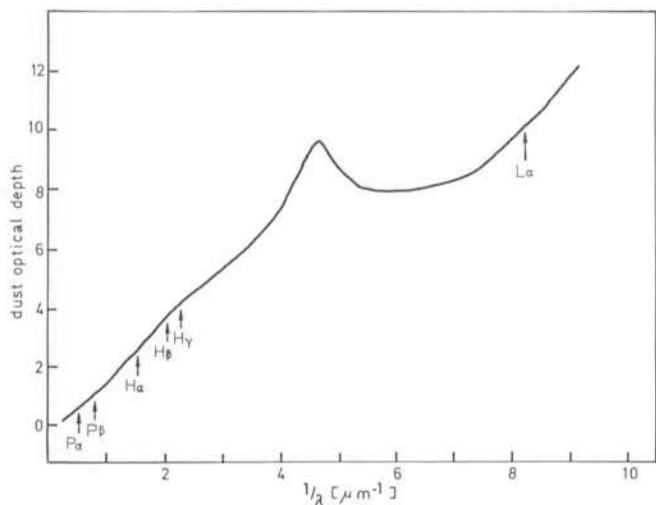


Fig. 2: Interstellar extinction curve for our Galaxy, as a function of reciprocal wavelength and with an arbitrary normalization. The wavelength positions of the main hydrogen lines in the infrared, optical and ultraviolet spectral ranges are indicated.

ed in order to make possible the spectrophotometry of IR lines in distant galaxies and quasars. Since 1980, with the beginning of period 26 at ESO, an InSb detector equipped with broad-band filters for photometry (1–5  $\mu\text{m}$ ) and with circular variable filters (CVF's) for narrow-band spectrophotometry (1.5–5.5  $\mu\text{m}$ ) became available at the ESO 3.6 m telescope (for details see the User's Manual by A. Moorwood and P. Salinari). The resolving power  $\lambda/\Delta\lambda$  of the CVF's ranges from 50 to 70. We were the first visiting astronomers at ESO who used this equipment. We applied it to measurements of the  $P\alpha$ -line strengths in active galactic nuclei.

The number of objects for which the Paschen lines are observable is strongly limited due to selective atmospheric extinction at IR wavelengths by the  $\text{H}_2\text{O}$  and  $\text{CO}_2$  molecules and for reasons of detector sensitivity as well as limiting apparent brightness of the sources themselves. In Fig. 3 the atmospheric transmission is plotted between 0 and 6  $\mu\text{m}$ . The

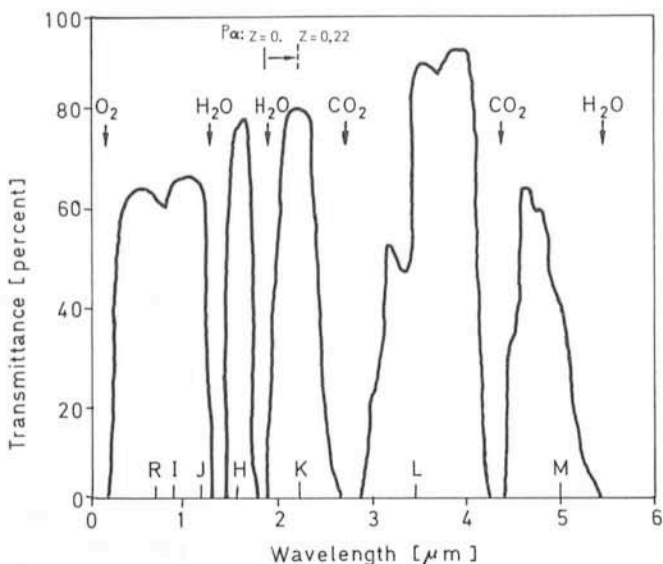


Fig. 3: The atmospheric transmission curve in the near and middle infrared as a function of wavelength. The infrared photometric bands are denoted by capital letters. The main absorbing molecules  $\text{O}_2$ ,  $\text{H}_2\text{O}$  and  $\text{CO}_2$  are responsible for the deep transmission gaps. The positions of an unshifted and a redshifted  $P\alpha$  line are also indicated.

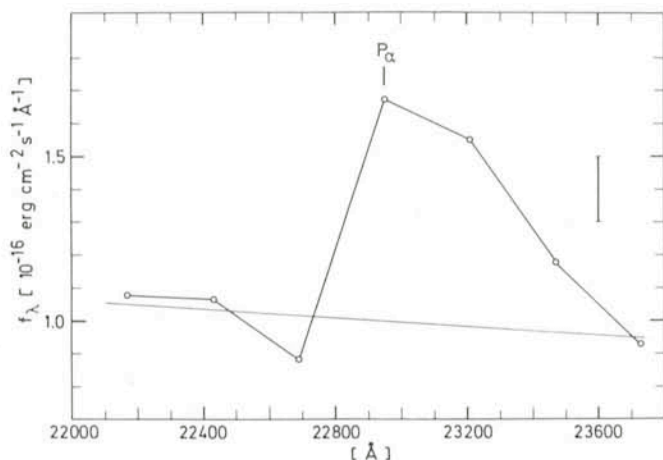


Fig. 4: The  $P\alpha$  line of the quasar PKS 0312-77 as measured with the InSb detector together with a circular variable filter at the ESO 3.6 m telescope.

rest wavelength of  $P\alpha$  falls right into an opaque band of our atmosphere. However, for the redshift range  $0.07 < z < 0.33$  of the sources the frequency of the  $P\alpha$  line is appropriately tuned in order to become observable in the adjacent frequency band, in which our atmosphere is much more transparent.

The location of the redshifted  $P\alpha$  line is indicated in Fig. 3 for the object PKS 0312-77. If both  $P\alpha$  and  $P\beta$  are to be observed simultaneously in the spectrum, the admissible redshift range is even smaller,  $0.23 < z < 0.33$ . Taking also into account the requirements of maximum exposure time and of visibility from La Silla, only 11 objects remain for  $P\alpha$  and  $P\beta$  observations out of the  $\sim 2,000$  objects contained in the lists of active nuclei and quasars (cf. e.g. M. P. Véron, P. Véron, 1974, "A Catalogue of Extragalactic Radio Source Identifications", *Astronomy and Astrophysics Supplement*, **18**, 309; A. Hewitt and G. R. Burbidge, 1980, "A Revised Optical Catalogue of Quasistellar Objects", *Astrophysical Journal, Supplement*, **43**, 57).

### 3. Results and Discussion

In our first run with the IR spectrophotometer at the ESO 3.6 m telescope in October 1980 we obtained  $P\alpha$  data for two objects: PKS 0312-77 and 3C 109. The first is a quasar with  $z =$

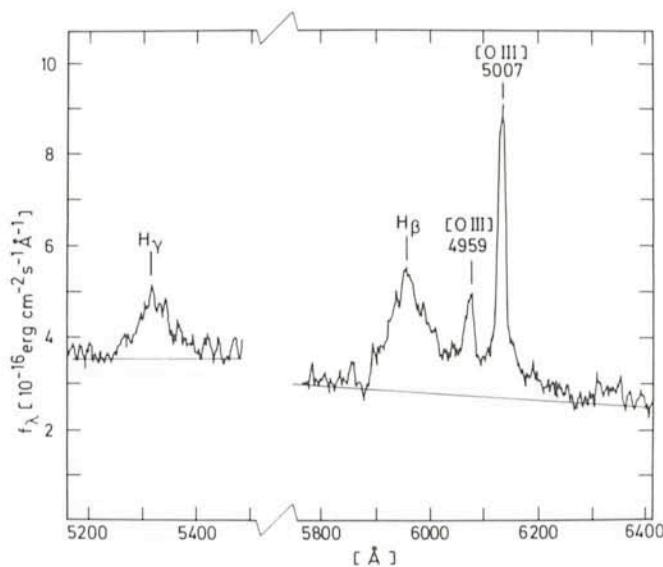


Fig. 5: Line profiles of  $H\gamma$  and  $H\beta$  for the quasar PKS 0312-77 as obtained with the image dissector scanner at ESO's 3.6 m telescope.

0.223, the latter a N galaxy having  $z = 0.306$ . We measured the profile at 7 equidistant wavelength positions symmetric around the expected line centre. We show in Fig. 4 the profile of the  $P\alpha$  line of the quasar; an estimated error bar is indicated. The accuracy of the profile compares favourably with  $P\alpha$  profiles obtained for some other objects by two American groups (Puetter et al., 1981, *Astrophys. J.*, **243**, 345; Soifer et al., 1981, *Astrophys. J.*, **243**, 369). During the same run we obtained Balmer line profiles with the Image Dissector Scanner attached to the Boller and Chivens spectrograph of the 3.6 m telescope. These are depicted for the same object in Fig. 5. The expected  $P\alpha/H\beta$  ratio from unmodified recombination theory is 0.35 (where a temperature of 10,000 K and opaque conditions are assumed). In our two objects we find comparatively enhanced values:  $1.24 \pm 0.3$  for the quasar and  $0.73 \pm 0.4$  for the galaxy. They are also higher than those found by Puetter and Soifer 1981 who find a range for this ratio from 0.09 to 0.72 for their sources with the exception of PG 0026+129, for which Puetter et al. found the very high ratio of 1.4 in 1978 (R. C. Puetter et al., 1978, *Astrophys. J., Lett.*, **226**, L53). The deviation from the recombination value may be explained by reddening in the sources and/or by optical depth effects. However, we think that the high  $P\alpha/H\beta$  ratios found by us indicate that the emission-line regions in nuclei are still poorly understood and substantial improvements in the line transfer calculations with and without dust absorption are necessary. Attempts in this direction are presently being done among others by R. C. Canfield and R. C. Puetter and by Mme S. Collin-Souffrin and collaborators.

Our observational results reported here are the subject of a more detailed paper (W. Kollatschny and K. Fricke, 1981, *Astron. Astrophys.*, in press). We are presently continuing our hydrogen-line observations in the infrared and optical spectral ranges using the ESO equipment and in the UV with the IUE

ANNOUNCEMENT OF AN ESO WORKSHOP ON

## The Most Massive Stars

ESO Munich, 23–25 November 1981

Among topics to be discussed in the workshop are the theory of evolution of massive stars, observations of luminous stars in the Galaxy and nearby systems, the effect of the presence of these stars on the structure and evolution of the interstellar matter in galaxies and their use as distance indicators.

The workshop will include both review papers and short contributions with ample time for discussion.

Contact address:

S. D'Odorico,  
Workshop on Massive Stars,  
ESO  
Karl-Schwarzschild-Str. 2  
D-8046 Garching bei München

satellite telescope in order to obtain complete sets of Lyman, Balmer and Paschen ratios for a sample of active galactic nuclei. We thus hope to provide useful constraints to improve the theoretical descriptions.

### Acknowledgement

This work was in part made possible by a grant (Fr 325/12 and Fr 325/15-2) of the Deutsche Forschungsgemeinschaft.

## UBV Photometry of Quasars

G. Adam, *Observatoire de Lyon*

### I. The Disappointed Hopes

#### 1. Hubble and the Birth of Observational Cosmology

Between the two world wars, a few people were, surprisingly, still concerned by extraterrestrial problems. One of them was Edwin Hubble, who discovered the so-called expansion of the universe, after proving the extragalactic nature of the great nearby spiral galaxies. Since then, astronomers have tried to understand the large-scale geometry of that newly opened universe. It is a long and still unsuccessful story. . .

How can we use the extragalactic objects to study that large-scale structure? There are two powerful methods:

(a) Counts of distant objects, up to some limiting magnitude. The dependence of the number of objects found on the radius sampled in the universe can in principle tell us if our universe is spherical and closed, or euclidean, or hyperbolic and open (a euclidean universe is just the kind of universe we like, with non-crossing parallels and circle area obeying the good old  $r$ -square law). In fact, the deceleration parameter  $q$  is the crucial one which defines the overall geometry.

(b) Plots of the recession velocity – or of the redshift  $z$  – of distant objects as a function of their measured luminosity. If we assume that the different objects have the same intrinsic luminosity, this is equivalent to a plot of the recession velocity versus the distance. Usually, one constructs a plot of  $\log z$

versus the apparent magnitude. For large values of  $z$ , the curves are very  $q$ -dependent and should tell us what is the "observational value", the one which fits best the experimental curves.

In fact, that approach initially failed: the most distant galaxies which can be observed are still too near to us, with  $z$  around 0.5. This is far too short an interval to allow a  $q$  determination.

#### 2. Quasars: The Cosmological Boom

In the early sixties, a new class of extragalactic objects entered the astronomical scene: the quasi-stellar objects, or quasars. Now, we have at hand lists of such objects which should soon reach the 2,000 entries, with large redshifts up to 3.53, and a lot of photometric measurements, mainly UBV. So it seems that solving the cosmological problem is just a matter of drawing a large Hubble diagram, fit a curve to the observational points, and write  $q$  in golden letters in the Great Book of Astronomical Achievements. But Figure 1, which is a Hubble diagram tying the B magnitude to the redshift for 358 quasars, has a most unpleasant look. . . The accuracy of modern UBV photometry is too high to account for such a scatter. In fact, there are three main difficulties:

(a) Use of the Hubble diagram assumes that all the objects observed have the same intrinsic luminosity. Unfortunately, this is very far from truth for quasars: at the same redshift, the

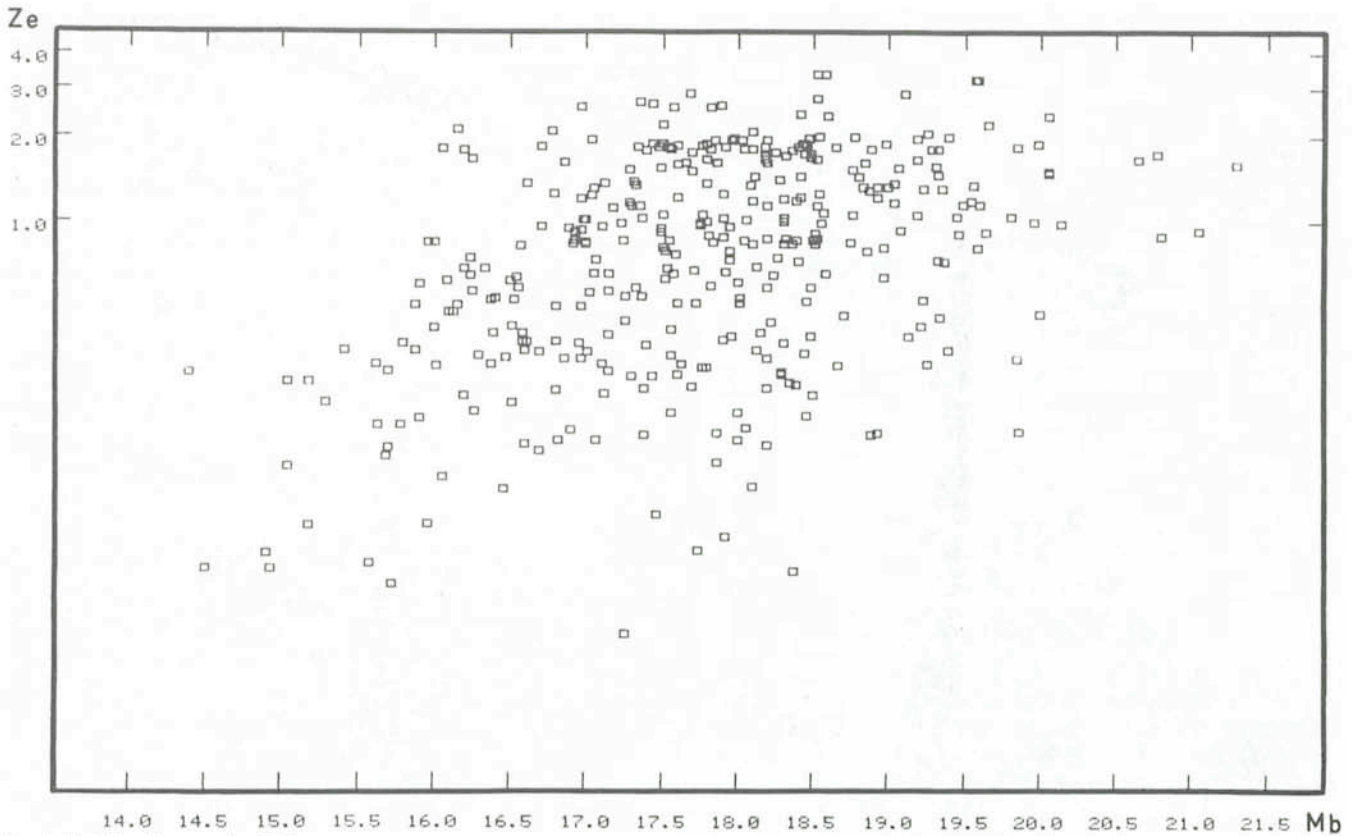


Fig. 1: Hubble diagram for 358 quasars.

magnitude of two objects can differ by several unities. More, a great number of objects are variable.

(b) At large redshifts, evolution effects become important, as we look at the objects as they were several billion years ago. And, up to now, we don't know which kind of evolution affects the quasars.

(c) The observational limits play very strongly in the high- $z$  part of the Hubble diagram. We work at the very end of the photometric possibilities of our telescopes, and selection effects are enormous. For instance, is the cut-off at  $z = 3.5$  real or due to some observational effects?

All this makes the Hubble diagram extremely difficult to work with. Great care must be taken in the statistical analysis.

## II. Why UB V Photometry?

It seems that UB V photometry doesn't give very useful information: due to the redshift, the spectral features falling into the U, B and V bands can be anything, varying from one object to another. Photometry with fixed bands is, then, a very coarse tool to study those exotic and complicated quasars. So, why waste astronomers' time doing UB V quasar photometry?

Well, there are a lot of things that just can't be done in an easier way than with UB V photometry:

### 1. Optical Identification of Radio Sources

Radio sources are usually detected without any aid from optical astronomy. It is then important to seek for optical counterparts, radio galaxies or quasars. This is done by exploring the vicinity of the radio source position on a deep sky photograph. When one finds a stellar object, it may be a star (and it is a misidentification) or a quasar. The ultimate proof will be a spectrum of the object. That is a long and costly operation, when the object is faint, which is the usual case.

It has been known, for a long time now, that quasar colours (the indexes U-B and B-V for instance) are different from the colours of ordinary stars. Figure 2 shows a plot of B-V versus U-B for the quasars. The observational points are represented as "bubbles", the diameters of which grow as  $z$ . In the early times of quasar studies, Allan Sandage found a fairly good correlation between the position of the representative point of a

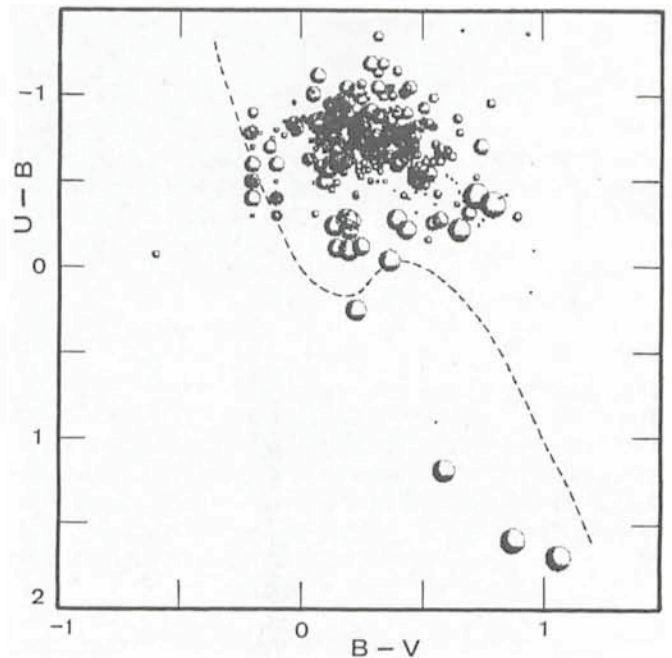


Fig. 2: Plot of U-B versus B-V for 384 quasars. The interrupted line is the Main Sequence for Galactic stars. Bubbles sizes vary as the redshift  $z$ .

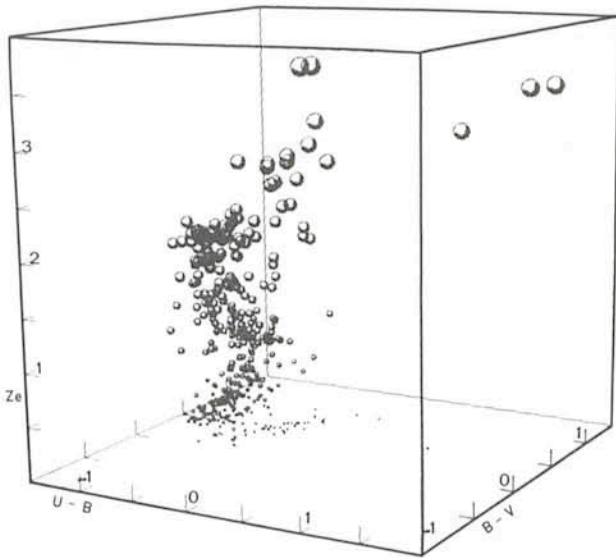


Fig. 3: Three-dimensional plot of U-B, B-V, and the emission redshift  $z_e$ . Bubbles sizes vary as  $z_e$ .

quasar and its redshift. This gave some hopes that the redshift determination may be replaced by a photometric UB-V measurement, a much faster operation. But Figure 2 shows that, as the z-range increased, the correlation disappeared. The early

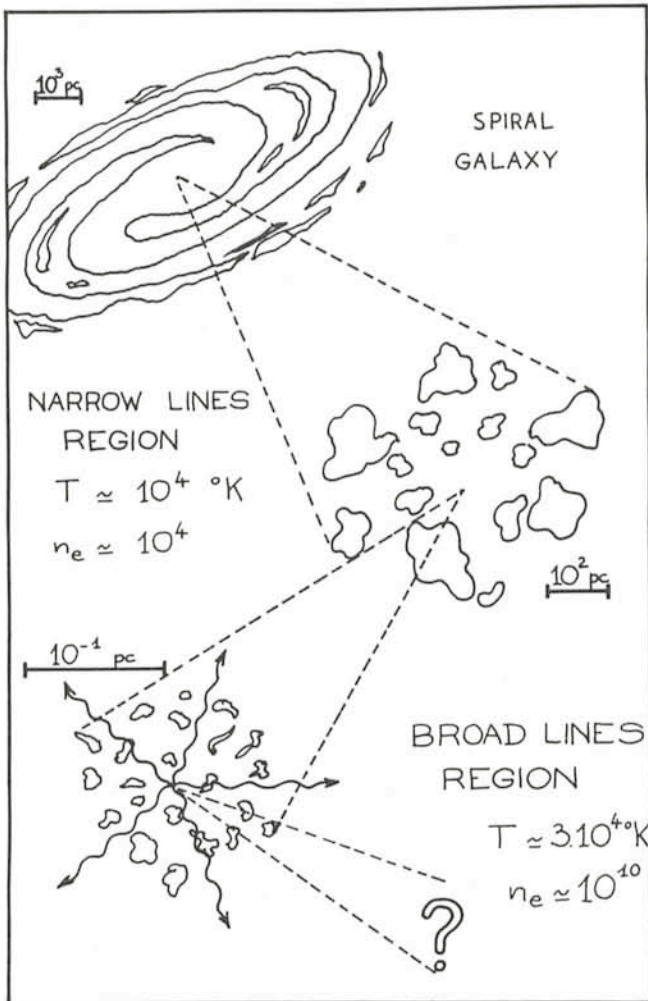


Fig. 4: Schematic view of a spiral galaxy with an active nucleus: one of these so-called quasars.

diagram of Sandage corresponds to the central over-crowded part of the present one. The very high redshift quasars are much "redder" and their representative points fall on the interrupted line where the bulk of the stars of the Galaxy are located. Figure 3, which is a three-dimensional plot including  $z$  as the third coordinate, shows that the U-B/B-V diagram is in fact the plane projection of a spiral path, and cannot be used alone.

Anyway, a quick UB-V measurement of a quasar candidate can tell us, at the 90% confidence level, if it is or not a quasar. The usual criterion is something like U-B lower than  $-0.35$ . Extremely few stars are so blue. So, it's good practice to use a middle-sized telescope for UB-V photometry before spending one hour on each object doing spectroscopy with a large instrument. The couple 1 m/3.6 m on La Silla is an excellent example of such an association.

## 2. Hubble Diagram of Quasars

Since the first attempts made to use that diagram, the situation has deeply evolved. The sample of quasars with known B or V magnitudes has enormously increased: more than 1,700 today (but with widely varying accuracies). Several hundreds were measured with the ESO 1 m photometric telescope. More, the multifrequency data are growing fast, in radio, infrared, ultraviolet, X-rays or gamma-rays. So, it is now possible to grapple with the problem in a new way: first, quasars are classified according to some observational characteristics (non-radio or radio, flat or steep spectrum, and so on...). Then, with those more homogeneous classes, one can try a new study of the sub-Hubble diagrams. This is part of the work in progress in Lyon. As it may be supposed that different classes of quasars correspond to different evolutive stories, these differences should show up in the sub-Hubble diagrams.

## 3. Quasar Physics

Figure 4 gives a very simplified view of a typical (as far as that exists) active nucleus of galaxy, such as a quasar. From centre to outside, one finds:

(a) The central "motor", not yet completely understood, but which could be an accreting giant black hole, that is a black hole swallowing pieces of stars torn apart by tidal forces, according to some promising models. This central motor produces an enormous amount of non-thermal radiation which is responsible for the energy transfer between the black hole system and the outer world.

(b) A region partially filled with filaments and clumps of hot (around 30,000 degrees) gas, with high velocities (between, say 1,000 and 10,000 km/s). The clouds are partially or totally ionized by the central continuum, and emit the very broad emission lines which dominate the classical quasar spectrum. This region has a diameter of the order of one parsec.

(c) Farther away (a few hundreds of parsecs), float large clouds of relatively cold (10,000 degrees) and diluted gas, less turbulent, which are responsible for the narrow lines seen in quasar spectra.

How can UB-V photometry help in the study of quasar physics? For instance, in two ways:

- It provides a quick manner of looking at the continuum emission. Figure 5 shows how the U-B index of quasars changes as the various emission lines are shifted across the photometric bands. For instance, one can see the change in colour around  $z = 2.5$ , where the very strong Lyman alpha emission line leaves the U band and enters the B band. So quasars with  $z$  greater than 2.5 look "redder". After making a UB-V measurement, one can correct for the emission-line

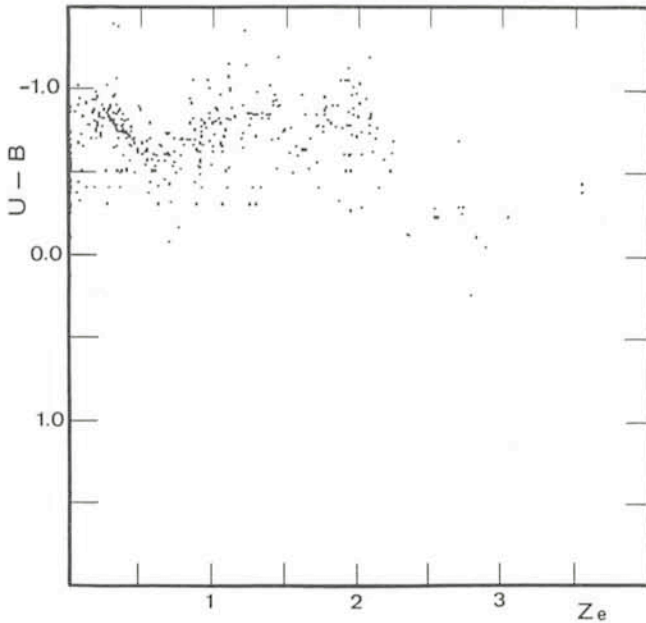


Fig. 5: Plot of  $U-B$  versus  $Z_e$  for 384 quasars.

influence by using a standard emission-line quasar spectrum, and get a good approximation of the slope of the continuum. Less accurate than spectrophotometry, of course, but far quicker. As quasars have usually the bad taste of being very

weak objects, a wide band photometry is essential to grasp a maximum of those scarce photons.

– The central regions of the nucleus emit, often, a variable amount of energy. The monitoring of that variability is the only way to get information about the sizes of the emitting regions. A simple argument shows that if an object is variable on a time scale of, say, a week, its overall dimensions cannot be much in excess of one light-week. Otherwise, variations concerning different parts of the object would be “averaged” and such a short time scale would not be observed. We are now reaching the day level, and that is, more or less, the lower limit the present models can accept. Discovery of faster variations in quasars would call for a new improvement of those models. So it is extremely important to seek for such fast variations, and to include such observations in a multifrequency programme. As radio, visible and X-ray radiations originate in different regions, multifrequency monitoring should throw new light on the structure of active galactic nuclei of galaxies.

The technical difficulties are great, of course: searching for fast variations, one searches for faint variations. Once again, broad band photometry is the good choice, with a large telescope and as many nearby standard stars as possible, to minimize the unavoidable noise.

What else? Well, we are, regarding the quasar problem, in the data-accumulation phase. Nobody can tell exactly what is a quasar, and it is still necessary to accumulate a maximum of information, and to seek for a maximum of correlations between parameters. It’s the time where people plot anything versus anything, and hope to find some New and Universal Truth. . . . Magnitudes are just one of such parameters.

## An Infrared Speckle Interferometer

*C. Perrier, ESO*

Since visible speckle interferometry has been developed ten years ago, efforts have been made to extend this technique to the infrared range for angular size measurements. Using the experience obtained on Kitt Peak by Sibille, Chelli and Lena (1979, *Astronomy and Astrophysics*, **79**, 315), an IR speckle interferometer has been developed at the La Silla observatory in connection with the installation of the IR photometer designed for the 3.6 m Cassegrain focus.

The aim of this article is to describe this system and to present the peculiarities of this observational technique in the light of selected results. But first let us recall the astrophysical motivation for such a work.

### The Need for High Resolution at IR Wavelengths

The main motivation is the lack of direct information on the spatial intensity distribution in existing models of the various objects belonging to the group of compact IR sources. Among them, those found in regions of active star formation are probably the most fascinating.

As all their flux is emitted in the infrared, ranging from a few microns up to hundreds of microns, these objects are not reachable with optical interferometry. On the other hand, their size may lie within the diffraction-limited resolution of the large telescopes: Fig. 1 shows the radius of a  $10 M_{\odot}$  protostar for three representative evolutionary times (taken from Yorke, 1980, *Astron. Astrophys.*, **85**, 215), assuming a diffraction-based limitation i.e. 0.12 arcsec at K (3.5  $\mu\text{m}$ ) and 0.27 arcsec at M (4.8  $\mu\text{m}$ ), we can see that this object, as far as 0.5 kpc, could be resolved at these wavelengths with a 3.6 m telescope.

Of course, other types of IR objects deserve an investigation at high resolution: IR/OH sources, giants or late-type stars with extended envelopes. For some Miras, size measurements at precise wavelengths corresponding to absorption features may reveal dynamical structures.

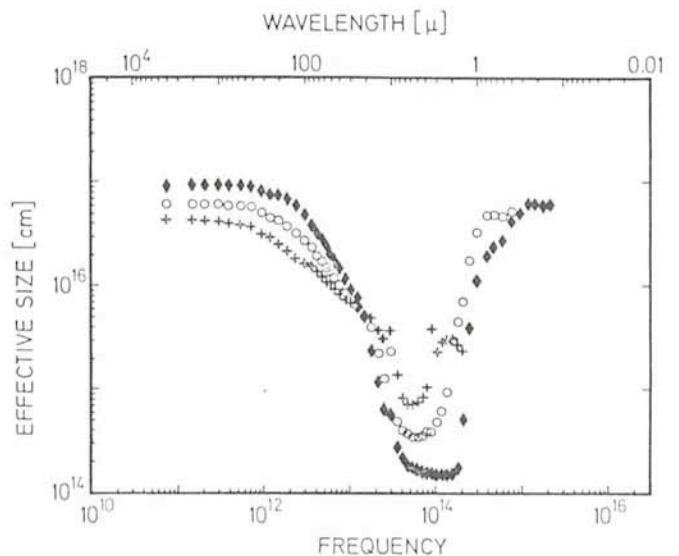


Fig. 1: Radius as a function of wavelength for a  $10 M_{\odot}$  protostellar object model at three evolutionary times. At K (2.2  $\mu$ ) and M (4.8  $\mu$ ) size is ranging from  $1.3$  to  $6.7 \cdot 10^4$  pc (from Yorke, 1980).

## Description of the System

Speckle interferometry has been described elsewhere before. The peculiarity of our system is essentially the use of a single detector because of the current lack of IR detector arrays.

### Method

The "specklemeter" is intended to achieve the full resolution of the telescope. Basically it takes and stores instantaneous images of the object. The short exposure of the astronomical image through the turbulent atmosphere freezes the turbulence and preserves, although attenuated, all the information at high resolution, given the pupil diameter  $D$  of the telescope.

In our one-dimensional case the image is scanned with a slit fitted to the optimum sampling step (width =  $\lambda/2D$ ). So the points of the resulting scan describe the intensity integrated over image cross-sections and contain all the spatial information along the selected direction of scanning. For freezing the temporal variations, each scan must be of the order of 10–30 ms.

Later on these data are reduced using Fourier transform techniques which allow such a line integral of the source brightness distribution to restore unambiguously a radial power spectrum, final output of the observations.

### Acquisition Chain

The system achieved at La Silla makes use of the standard InSb photometer (Fig. 2, modified from 3.6 m IR Photometer User's Manual, A. Moorwood and P. Salinari, 1980). The wavelength range of interest, 2.2–4.8  $\mu\text{m}$ , is covered by its standard narrow-band filters. Thanks to the IR team in Geneva, some modifications not necessary in photometric mode were included from the beginning, like the use of an off-axis mirror corrected for aberrations and the design of a high-frequency boosted preamplifier. The photometric wobbling process being replaced by scanning, the focal plane wobbling mirror receives here a saw-tooth drive signal.

Due to the high-speed sampling of each scan, a special electronics chain had to be built. With a typical scanning time of

10 ms and a 2 arcsec seeing, the time per scan point is 150  $\mu\text{s}$ . The usual way to read the data from an ESO instrument would result in prohibitive delays (2 ms) between successive readings. In order to avoid building a complex specific module, the chosen solution, as found by Mr. D. Hofstadt, consists in overriding the computer control to allow direct access to the instrument interface (the Camac module). This somewhat delicate operation has proved to be reliable enough to provide an efficient remote control of the instrument thanks to Mr. M. Maugis who succeeded in making the whole chain error-proof and performant. The only drawback is to prevent the computer from being full time accessible; nevertheless, this effect remains hardly visible.

A scope helps for optimizing the signal when the object is not too faint, otherwise a lock-in amplifier, as used in photometry, must be preferred. But both may be necessary for day-time guiding which has been successfully achieved this way.

### Software

The general ESO philosophy, consisting in providing highly interactive programmes, has been followed. As a matter of fact, speckle observations require much effort on the software side because monitoring the incoming data and doing on-line reduction are important requirements. This is mainly due to the almost always variable seeing conditions which lead us to permanently wonder whether some observing parameters should not be modified. In order to make this frequent optimization feasible, and given the fact that the instrument in the Cassegrain cage gets sometimes inaccessible, remote control commands were implemented together with graphics routines and reduction facilities.

The latter are challenging operations for the ESO HP 21 computer which shows here its true limitation. We overcame this obstacle by reducing on-line an amount of data smaller than available, knowing that we were rather lucky to succeed in doing so, whereas this would be impossible with two-dimensional data.

### Compatibility with Photometry

One may be tempted to mix both modes (photometry and speckle) in a same night. But the compatibility seems fairly low between the two set-ups. Mr. H. Kastowski managed to make exchanges feasible without waste of precious observing time by designing separate permanent cablings. But still any exchange requires the modification of the scanner setting and possibly the exchange of the HF boosted preamplifier not suited for usual photometric measurements. So sharing time between the two modes have usually been avoided, even if both corresponding programmes which run under the same executive system can be interchanged without loss of data.

## Examples of Results

The first observations on La Silla were performed in 1980 and since then a number of objects of interest have been observed, mainly at 4.8  $\mu\text{m}$  because of their strongly reddened colours. In addition to, properly speaking, astrophysical results, a large amount of information concerning the atmospheric behaviour has been obtained and should be useful for a better understanding of the seeing quality at the 3.6 m.

### Limiting Magnitudes

Typical individual scans are plotted in Fig. 3: the scanning rate was 9.5 ms for 64 points corresponding to 5.6 arcsec on

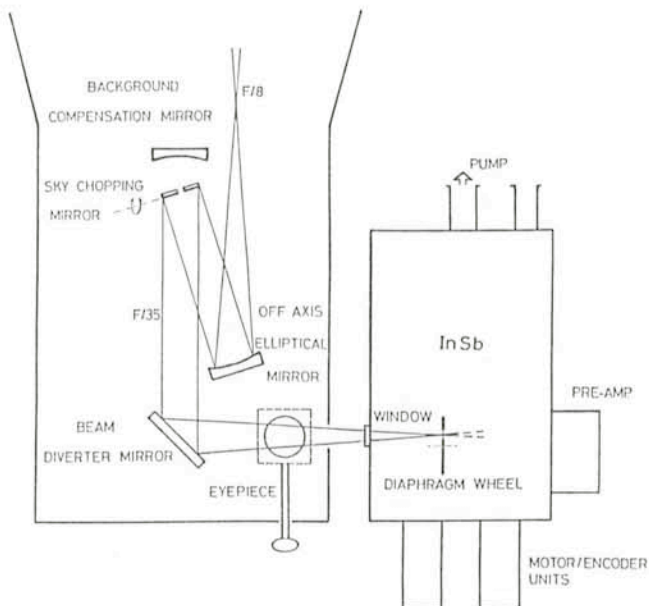


Fig. 2: Optical configuration of the IR photometer adaptor (see also 3.6 IR Photometer User's Manual).

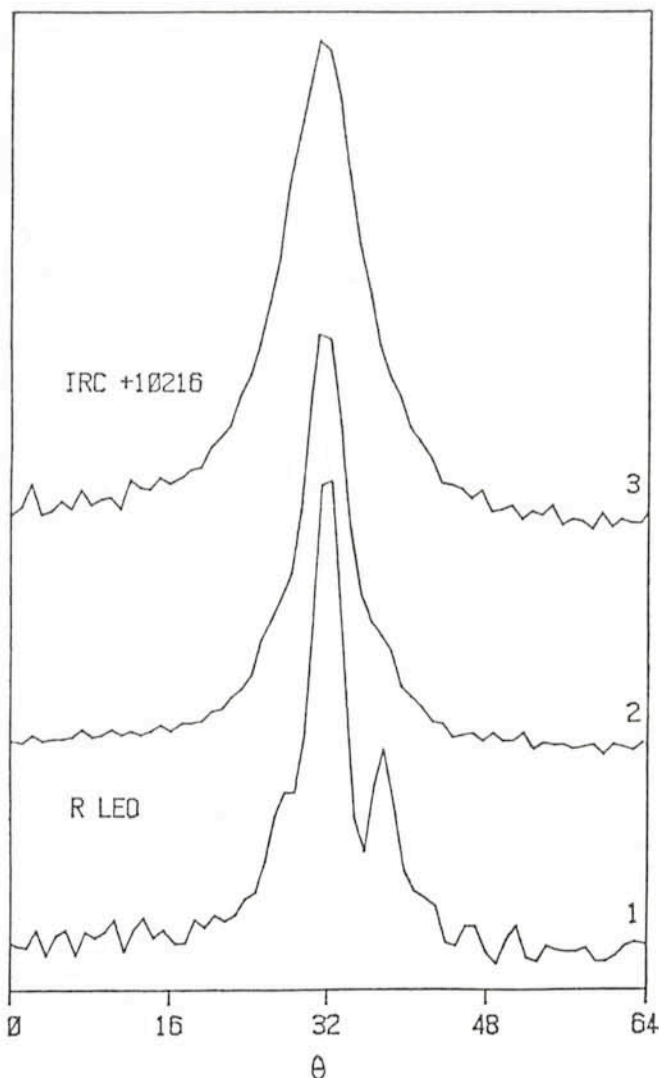


Fig. 3: Scans obtained in band M with the ESO 3.6 m telescope in October 1980. Sampling period: 87 milliarcsec.

1 – Point-like source, the 10 ms scan shows speckles.

2 – Same scan as 1 averaged with following ones during 180 ms, speckles are smoothed out.

3 – Extended object, the 10 ms scan exhibits no speckles at all.

the sky. So the maximum sampling frequency ( $5.7 \text{ arcsec}^{-1}$ ) was larger than the telescope cut-off frequency ( $3.72 \text{ arcsec}^{-1}$  at M) as is preferable for securing an oversampling.

Both objects are late-type stars with negative K and M magnitudes. So these graphs do not represent the usual appearance of individual scans of common and less bright objects. But one can deduce from them the limiting magnitudes  $M_{\text{lim}}$  in speckle mode and compare to the known photometric performance. With one arcsec seeing, one finds  $M_{\text{lim}} (3\sigma, 1s) = 4$  in agreement with  $M_{\text{lim}} = 3.4$  derived from  $M_{\text{lim}} (3\sigma, 15mn) = 10$  given for the photometric mode with a 3 arcsec diaphragm. The slight discrepancy – favourable for speckle mode – comes from the background limitation in photometry, no longer present in the speckle mode where the instrument throughput is reduced. Similarly the same deduction leads to  $K_{\text{lim}} (3\sigma, 1s) = 8$ .

$M_{\text{lim}} (1s)$  only gives the limitation in the guiding sense when the signal is used for centring; if offset guiding is achieved on field stars, a longer integration is possible, hence fainter objects may be analysed.

### Object Spectrum

The final object spectrum contains information on the size of the object up to the cut-off frequency  $D/\lambda$  of the telescope. This makes the value of speckle interferometry obvious even when a single cross-section of the object spectrum is obtained. Such a spectrum is shown in Fig. 4: IRC + 10216 is a carbon star with double shell structure. Because of the non-unicity of the solution describing complex structures in the image, the radial intensity distribution cannot be retrieved in a straightforward way, except on bright objects, where the high signal-to-noise ratio should allow the use of phase-restoration techniques, still in their infancy when applied to astrophysical data.

But one can assert the departure of the object from circular symmetry by exploring different directions of scanning. This explains that we often rotated the Cassegrain adaptor for observing some interesting objects expected to present some asymmetry. This feature offered by the 3.6 m Cassegrain focus is indeed an important advantage of the system configuration.

## A Useful New Catalog

**A revised Shapley-Ames catalog of bright galaxies** by Allan Sandage and Gustav Tammann has just been published by the Carnegie Institution of Washington.

In 1932, Shapley and Ames published their Harvard survey of 1,246 bright galaxies. Their work became the basic listing of bright galaxies; after half a century, it still has a major role in studies of galaxies in the local region.

In the early 1950's, Sandage set out a plan to compile type, magnitude, and redshift data for all galaxies in the original Shapley-Ames catalog. The project, later joined by Tammann, was an outgrowth of the photographic survey of bright galaxies begun at Mount Wilson in 1909 and continued at Palomar after completion of the 5 meter Hale telescope in 1949.

The result of that long-range program is the present catalog, containing data on types and magnitudes for all the Shapley-Ames galaxies and redshift for all but one (NGC 3285). The usefulness of this catalog lies mainly in the list of uniformly determined Hubble type for a large and complete sample of galaxies. Too often, in the literature, the

type of galaxies has been estimated on poor photographs producing unexpected results. But another aspect of this work makes it a necessary tool for all astronomers interested in bright galaxies: the listed redshifts are extracted from 430 sources. For 68% of all galaxies, at least two independent redshift determinations are available, but the velocity of 394 galaxies rests on only one determination and could be in some cases in error. However, it is estimated that the median error is  $40 \text{ km s}^{-1}$ .

The book also contains 90 illustrations of galaxies exemplifying luminosity classes.

This catalog is a necessary tool as it provides a uniform set of basic data for a large and complete sample of nearby galaxies. It can be ordered from:

Publications office  
Carnegie Institution of Washington  
1530 P Street, N.W.  
Washington, D.C. 20005

Its price is 29 US\$.

P. V.

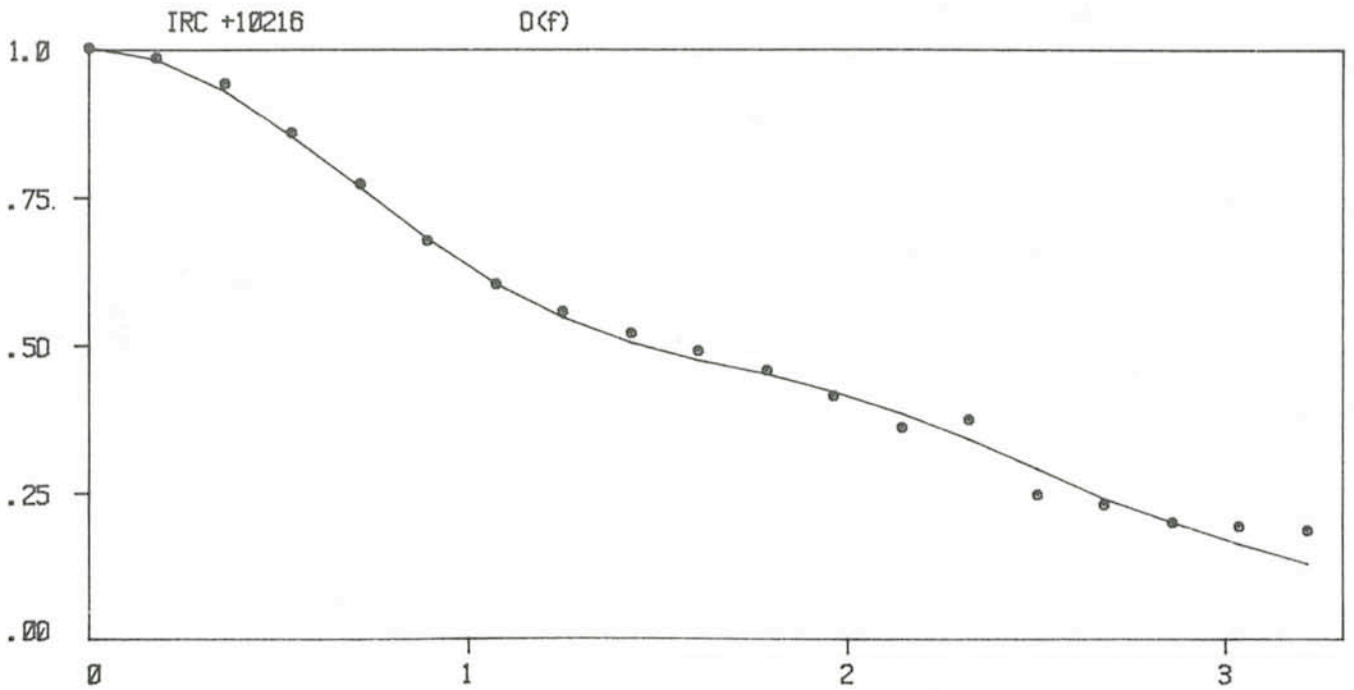


Fig. 4: Spectrum modulus of IRC + 10216 (normalized at origin, versus spatial frequency in arcsec<sup>-1</sup> at L(3.5  $\mu$ )). Scanning direction is east-west. The full line represents a model composed of two disks of 0.36 and 1.2 arcsec respective diameters.

### Seeing Variations

The critical step in the "image modulus" restoration process is to determine the atmospheric coherence length, parameter correlated to the seeing and theoretically retrievable from the data themselves. This parameter appears to be of prime importance when one corrects the reduced data from the point-spread function as measured on a point-like source, hence with other seeing conditions than with the object. But this task is increasingly difficult as the source becomes fainter because it makes the computation less and less reliable. The only way to avoid this artificial limitation to a correct restoration is to

measure the seeing independently through a "seeing monitor" centred on a field star.

As evidence has been given that such an instrument should be included in a more general seeing study (R. Wilson, 1980, ESO internal report on dome seeing), we have good hope to add a prototype soon into the speckle system.

I wish to thank A. Moorwood and P. Salinari for the introduction to the new IR photometer and the ESO electronic staff of La Silla for the repetitive support they gave to transform an unorthodox project into reality.

## Photometric Classification of Pulsating Variables with Periods between One and Three Days

R. Diethelm, *Astronomisches Institut der Universität Basel*

The MESSENGER contains many articles referring to exciting celestial objects of more or less "exotic" nature. In this note the description of the photometric behaviour of only a small group of stars is presented, which nevertheless have proven to be important in the quest for measuring distances, and which may hold keys for the theory of stellar evolution. These stars show periodic variations of their apparent brightness due to a radial pulsation instability of their outer atmospheres. Commonly they have been divided into two major subgroups, the RR Lyrae stars whose periods lie between a few hours and roughly one day, and the Cepheid variables with periods of more than one day. While the first – also called cluster-type variables – are considered to be members of the

oldest stellar population of our Galaxy, the latter are thought to belong primarily to the younger stellar population.

It has been shown during the first decennia of this century, that the RR Lyrae stars all have roughly the same intrinsic brightness, while the Cepheid variables satisfy a proportionality between their absolute magnitude and the logarithm of their period. These facts render them powerful distance indicators within our own galaxy, at least on our side of the galactic nucleus and in some cases even to our nearest neighbour galaxies.

The division of the two major subgroups at a fixed period is quite arbitrary and not supported by any physical considerations. In fact, some overlap in the period interval between one

and three days has been found long ago. A simple method to distinguish the members of the two groups is therefore desired.

## Classification

With this aim in mind, an investigation of all the available photoelectric lightcurves was undertaken, and in a number of cases, new photometry was secured. Very useful in this investigation were the measurements obtained by Dr. K. K. Kwee and Dr. G. A. Tammann in recent years at the ESO 1 m telescope on La Silla. These data proved to be of excellent quality and showed that simple UBV photometry yields an unequivocal classification scheme. As it turned out, no less than five different types of pulsating variables with periods between one and three days can be observed. These five subgroups are illustrated in Figure 1 by the V lightcurves of one representative of each subgroup; a short description of the main lightcurve characteristics is as follows:

(1) *RR Lyrae stars*: The rise from minimum to maximum takes only about one tenth of the period. The overall variation is very smooth with only a small hump before minimum light. Very typical is the fact that the U-B curve shows a decrease while the V brightness is increasing. According to these criteria UX Nor with a period of 2.4 days is the longest-period RR Lyrae star known.

(2) *"CW" stars*: A secondary hump of considerable amplitude – in the order of one third of the whole amplitude – is found prior to the primary maximum. The representative of this class with the shortest known period is HQ CRA ( $P = 1.415$ ).

(3) *BL Herculis stars*: The main feature of this subclass is the existence of a hump on the descending branch of the lightcurve, which leaves the impression of a "flat-topped" or "shouldered" curve. In the period interval 1–3 days only 5 galactic representatives of this class are known.

(4) *Classical Cepheids*: The lightcurve is very smooth, but the rising portion covers a larger fraction of the period than the one for RR Lyrae stars. There seems to exist no star in this group whose period is less than two days; in fact the galactic Classical Cepheid with the shortest period known is BB GEM ( $P = 2.308$ ).

(5) *Sinusoidal Cepheids*: As implicated by the name of this subclass, its members show almost sinusoidal variations with only a small amplitude. This subgroup contains the brightest stars in the present sample, which is mainly due to a selection effect.

## Conclusions

The galactic pulsating variables with periods between 1 and 3 days and with sufficient photometry can all be assigned to one of the above subgroups. The classification scheme is further supported by the different behaviour of these stars in the (U-B) versus (B-V) plane during their light cycle, and it is compatible with the spectroscopic data so far available. This does not necessarily call for a physically meaningful division of these stars. However, their distribution in the Galaxy, the occurrence of some of them in globular clusters, their counterparts in the Magellanic Clouds as well as other observational and theoretical investigations, all support the view that the present classification separates real physical differences. As to the nature of the different subgroups the following conclusions are indicated:

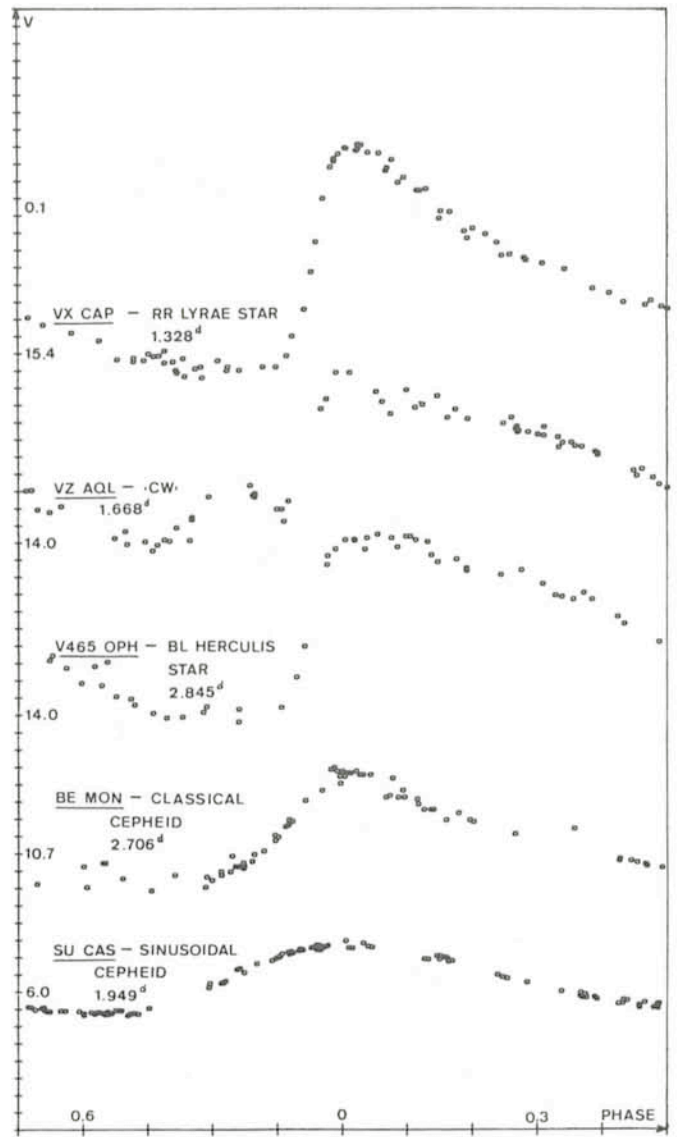


Fig. 1: Examples of V lightcurves of the five proposed subclasses of Cepheid variables with periods between one and three days. Observations were obtained by K. Kwee (AA Suppl., 2, 77, and private communication) for VX CAP, VZ AQL and V465 OPH; by G. A. Tammann (private communication) for VZ AQL and V465 OPH; by Buchanowa et al. (IBVS 727) and by Szabados (Mitt. Stw. Ung. Akad. d. Wissensch., Nr. 70) for BE MON and finally for SU CAS by Milone (IBVS 482).

(a) RR Lyrae stars are old, metal-deficient, low-mass stars and their distribution and kinematical properties prove them to be members of the halo population.

(b) BL Herculis and "CW" stars are closely related to the W Virginis stars of longer periods. The distribution of the members of the two groups in our Galaxy is different. "CW" stars are more concentrated towards the galactic plane and seem to be confined to the galactic centre region. They must be considered as intermediate, respectively old disk population constituents. The differences in their lightcurves are probably due to different chemical composition, mass and hence evolutionary history.

(c) Classical Cepheids and sinusoidal variables are young, massive disk objects. While the Classical Cepheids vary in their fundamental pulsation mode, the Sinusoidal Cepheids are pulsating in the first overtone mode. The theoretical period ratio

between fundamental and first-overtone pulsations is 1 : 0.71 for Cepheids; the observed short-period cutoff at  $P = 2.3$  days (BB GEM) and  $P = 1.95$  days (SU CAS) respectively, is therefore in good agreement.

For pulsating variables the period interval from 1 to 3 days is a twilight zone, where distinctly different types of variables coexist. Their observational separation is a necessary first step for a deeper understanding of their physical parameters and their evolutionary status.

## List of Preprints

### Published at ESO Scientific Group

#### June – August 1981

151. M. W. Pakull: HD 36705 – A New Bright X-ray Emitting RS CVn Star. *Astronomy and Astrophysics*, Letters. June 1981.
152. J. Krautter, G. Klare, B. Wolf, H. W. Duerbeck, J. Rahe, N. Vogt and W. Wargau: IUE Spectroscopy of Cataclysmic Variables. *Astronomy and Astrophysics*, Main Journal. June 1981.
153. J. R. Dickel, S. D'Odorico, M. Felli and M. Dopita: Detection of Radio Emission from Optically Identified SNR in M31. *Astrophysical Journal*. June 1981.
154. A. Lauberts, E. B. Holmberg, H. E. Schuster and R. M. West: The ESO/Uppsala Survey of the ESO (B) Atlas of the Southern Sky. IX. *Astronomy and Astrophysics*, Supplement Series. June 1981.
155. J. Lequeux and R. M. West: Preliminary Stellar Photographic Photometry in the Sculptor Dwarf Irregular Galaxy (SDIG). *Astronomy and Astrophysics*, Main Journal. July 1981.
156. R. Barbier: Ultraviolet Colours of Early-type Stars. *Astronomy and Astrophysics*, Main Journal. July 1981.
157. E. A. Valentijn: Westerbork 5 GHz Observations of Head-Tail Radio Sources in A2022, A2256 and A2462. *Astronomy and Astrophysics*, Main Journal. July 1981.
158. D. Baade: An Unusually Short Stable Period of Absorption Line Asymmetries and V/R Variations in the spectrum of the Be Star 28 CMa. *Astronomy and Astrophysics*. July 1981.
159. G. Contopoulos: The Effects of Resonances Near Corotation in Barred Galaxies. *Astronomy and Astrophysics*. July 1981.
160. R. M. West and R. Barbier: The Very Large, Interacting Galaxy Pair IC 5174/75. *Astronomy and Astrophysics*, Main Journal. July 1981.
161. N. Vogt and F. M. Bateson: An Atlas of Southern and Equatorial Dwarf Novae. *Astronomy and Astrophysics*, Supplement Series. July 1981.
162. J. Koornneef: The Gas to Dust Ratio and the Near-infrared Extinction Law in the Large Magellanic Cloud. *Astronomy and Astrophysics*, Main Journal. July 1981.
163. G. Contopoulos, P. Magnenat and L. Martinet: Invariant Surfaces and Orbital Behaviour in Dynamical Systems of 3 Degrees of Freedom. II. *Physica D. Nonlinear Phenomena*. August 1981.
164. H. Arp and J. Surdej: Quasars in a Control Field Far from Bright Galaxies. *Astronomy and Astrophysics*. August 1981.
165. P. Véron and M. P. Véron: On the Quasar Surface Density. *Astronomy and Astrophysics*. August 1981.
166. P. A. Shaver, V. Radhakrishnan, K. R. Anantharamaiah, D. S. Retallack, W. Wamsteker and A. C. Danks: Anomalous Motions of HI Clouds. *Astronomy and Astrophysics*, Letters. August 1981.
167. S. D'Odorico, W. M. Goss and M. A. Dopita: Radio Emission from Supernova Remnants in the Galaxy M33. *Monthly Notices of the Royal Astronomical Society*. August 1981.
168. A. Surdej, J. Surdej and J.P. Swings: Spectral Variations and Evidence for Edge and/or Line Locking Mechanism(s) in the Low Excitation Planetary Nebula HD 138403. *Astronomy and Astrophysics*, Main Journal. August 1981.

## PERSONNEL MOVEMENTS

### STAFF

#### Arrivals

##### Europe

- MORESMAU, Michel, F. Electronics Technician, 24.8.1981  
 KÄSLING, Angelika, D. Administrative Clerk, 1.9.1981  
 LECLERCQZ, Jean-Marie, B. Draughtsman (Graphics), 1.9.1981  
 LIZON À L'ALLEMAND, Jean Louis, F. Opto-mechanical Technician, 15.9.1981  
 MISCHUNG, Norbert, D. Senior Project Engineer, 1.11.1981  
 DEKKER, Klaus, NL, Head of Optical Section, 1.11.1981

##### Chile

- RUBLEWSKI, Wilhelm, D, Senior Electronics Technician, 1.9.1981

#### Departures

##### Chile

- ESCHWEY, Jörg, D, Head of Construction Group, 31.12.1981

### ASSOCIATES

#### Arrivals

##### Europe

- MILLER, Richard H., USA, 1.9.1981

#### Departures

##### Europe

- GLASS, Ian, Irish, 30.9.1981

### FELLOWS

#### Arrivals

##### Europe

- SVENSSON, Roland, S, 1.10.1981

### ALGUNOS RESUMENES

## ESO fue seleccionada para alojar el servicio de coordinación europea del telescopio espacial

La "National Aeronautics and Space Administration" (NASA) de los Estados Unidos intentará lanzar un telescopio espacial de 2.4 m hacia fines de 1984. En este proyecto participa la Agencia Espacial Europea (ESA), y los observadores de los países miembros de esta institución obtendrán por lo menos un 15% del tiempo total de observación con el telescopio espacial.

El día 26 de junio ESO fue elegida por ESA para alojar el servicio de coordinación del telescopio espacial.

Las tareas más importantes del servicio de coordinación serán:

- dar informaciones sobre programas de observación a posibles observadores;
- coordinar el desarrollo del software para el análisis de los datos y crear software adicional para responder a las demandas de la comunidad europea del telescopio espacial;

ESO, the European Southern Observatory, was created in 1962 to . . . establish and operate an astronomical observatory in the southern hemisphere, equipped with powerful instruments, with the aim of furthering and organizing collaboration in astronomy . . . It is supported by six countries: Belgium, Denmark, France, the Federal Republic of Germany, the Netherlands and Sweden. It now operates the La Silla observatory in the Atacama desert, 600 km north of Santiago de Chile, at 2,400 m altitude, where twelve telescopes with apertures up to 3.6 m are presently in operation. The astronomical observations on La Silla are carried out by visiting astronomers – mainly from the member countries – and, to some extent, by ESO staff astronomers, often in collaboration with the former. The ESO Headquarters in Europe are located in Garching, near Munich. ESO has about 120 international staff members in Europe and Chile and about 150 local staff members in Santiago and on La Silla. In addition, there are a number of fellows and scientific associates.

The ESO MESSENGER is published four times a year: in March, June, September and December. It is distributed free to ESO personnel and others interested in astronomy. The text of any article may be reprinted if credit is given to ESO. Copies of most illustrations are available to editors without charge.

Editor: Philippe Véron  
 Technical editor: Kurt Kjær

EUROPEAN  
 SOUTHERN OBSERVATORY  
 Karl-Schwarzschild-Str. 2  
 D-8046 Garching b. München  
 Fed. Rep. of Germany  
 Tel. (089) 32006-0  
 Telex 05-28282-0 eo d

Printed by Universitätsdruckerei  
 Dr. C. Wolf & Sohn  
 Heidemannstraße 166  
 8000 München 45  
 Fed. Rep. of Germany

- archivar y catalogar todas las observaciones realizadas con el telescopio espacial y mantener éstas a disposición de los científicos europeos;
- dar facilidades para la reducción de datos obtenidos con el telescopio espacial a los observadores europeos.

## Una noche de observación vista desde otro ángulo

Para el personal técnico de La Silla significa un gran desafío tratar con equipos experimentales y únicos, en vez de con aquellos instrumentos bien comprobados que ya se encuentran en el mercado. Pero a la vez significa un arte tratar con una especie humana muy especial que es ciertamente única y peculiar: el astrónomo.

La evolución en la tecnología instrumental ha maltratado bastante al observador. Hoy en día usa toda clase de sofisticados artilugios técnicos para coleccionar sus fotones y, a veces, éstos arruinan su programa. Pero el factor más incómodo en todo esto es el hecho de que está participando más y más en el campo de la observación un hombrecito que crece en importancia: el hombre de la mantención.

Durante la noche cuando falla el instrumento se desencadena un infierno al lado del telescopio. Se adentra en la cúpula un temeroso hombrecito con una caja colorada. Confrontado inmediatamente a un sinnúmero de contradicciones deberá hacerse su camino para encontrar una sólida evidencia de la

falla. Se verá asaltado por una tormenta de acaloradas preguntas y quejas:

¿Cómo es que ha venido tan tarde?  
 ¿No podrías haberse prevenido esto?  
 ¿Cuánto tiempo tomará para arreglar el problema? ¿Qué es lo que no funciona?

¡Si solamente supiera! El hombrecito trata de contenerse. Sabe que debe permanecer tranquilo e inspirar confianza, ya que el astrónomo no le creará en supremo acto de confianza. Sobre todo deberá presentar herramientas y actividad. No hay tiempo para pensar con calma o estudiar el problema en un lugar tranquilo; se requiere su presencia física. Pues si no tendría que afrontar intromisiones, mal genio, voces altas e incluso malas conductas.

Las noticias se divulgan por la montaña y varias caras desconocidas ya andan husmeando, comentando el suceso, comentando el servicio, comentando la organización.

Gregario consuelo para las víctimas mientras que el hombrecito sigue pegado a la máquina. Frente a él luces centelleantes se niegan a revelar su secreto; detrás una cara tensa y nerviosa le hace más preguntas. Poco a poco comienza a sentir que lo dominan pensamientos blasfemos.

Y al fin localiza la pizca de polvo y el instrumento comienza a traquetear nuevamente.

El hombrecito se retira, aliviado, con un peso menos encima del corazón . . . hasta que nuevamente lo llame el "pip, pip".

*D. Hofstad*

## Contents

D. Hofstad: An Observing Night as Seen from the Other Side . . . . .	1
The European Coordinating Facility for the Space Telescope . . . . .	1
I. Appenzeller, O. Stahl and B. Wolf: The Hubble-Sandage Variable HDE 269006: A Hot Supergiant with a Cool Envelope . . . . .	2
Tentative Time-table of Council Sessions and Committee Meetings . . . . .	3
Applications for Observing Time at La Silla . . . . .	5
M. Imbert and L. Prévot: First Observations with CORAVEL at La Silla . . . . .	6
New Head of the Scientific Division . . . . .	7
W. K. Huchtmeier, O.-G. Richter and J. Materne: Clusters of Galaxies . . . . .	8
M. Aurière: Structure of the Core of Globular Clusters . . . . .	12
ESO Council Decision . . . . .	13
Visiting Astronomers . . . . .	14
C. Madsen: Non-Atlas Photographic Work in the ESO Sky Atlas Laboratory . . . . .	16
J. Krautter and G. Gahm: Do T Tauri Stars Have Extensive Coronae? . . . . .	19
Proceedings of the ESO Conference on "Scientific Importance of High Angular Resolution at Infrared and Optical Wavelengths" Now Available . . . . .	21
K. J. Fricke and W. Kollatschny: Paschen and Balmer Lines in Active Galactic Nuclei . . . . .	21
Announcement of an ESO Workshop on "The Most Massive Stars" . . . . .	23
G. Adam: UBV Photometry of Quasars . . . . .	23
C. Perrier: An Infrared Speckle Interferometer . . . . .	26
A Useful New Catalog . . . . .	28
R. Diethelm: Photometric Classification of Pulsating Variables with Periods between One and Three Days . . . . .	29
List of Preprints Published at ESO Scientific Group . . . . .	31
Personnel Movements . . . . .	31
Algunos Resúmenes . . . . .	32